CHAPTER 4

MARINE DISCHARGES

The most common way of disposing waste into the sea is to discharge it by means of submerged outfalls, which consist basically of a pipe with one or more discharge ports. The initial behaviour of the released effluent depends almost exclusively on the values at the source of some relevant fluxes (momentum, mass and buoyancy), and on the orientation and geometry of the ports; further away, several environmental factors will act upon the released fluid, and will therefore govern the subsequent behaviour of the plume.

The present chapter deals with the description of the possible phases that a marine discharge may experiment –i.e., pure jet, pure plume and buoyant jet phases- until the density of the discharge and that of the receiving water become similar, and presents the effects of waterbody stratification and ambient currents on the discharge. The last section introduces the different regions into which the dispersion process is commonly divided, and gives a description of each one. Although the present description is based on marine outfalls, the underlying theory is applicable to general discharges into coastal waters, such as rivers and thermal effluents.

4.1 FLOW DISCHARGES INTO A WATERBODY

Due to the large number of variables affecting the behaviour of an outfall discharge into a waterbody, the initial dilution and other characteristics of the resulting wastefield are generally very difficult to determine. Therefore, most of the studies and analyses available in the literature are concerned only with limiting cases, such as those of a single (or fully merged) jet or plume in simplified environments (uniform or linearly stratified watercolumn, currents parallel or normal to the discharge direction, etc). The usual approach in these studies is to apply dimensional considerations

and lengthscale arguments to the study case, based on the fluxes of momentum, volume and buoyancy, and then compare the results with data obtained either from field measurements or from controlled laboratory experiments.

The initial behaviour of the effluent ejected from an outfall is generally governed by the discharge momentum, although the density difference with respect to the receiving waterbody creates vertical buoyancy forces which tend to force a vertical motion of the fluid. Under these circumstances, the discharge acts as a buoyant jet. The decay in momentum is faster than the decrease in the density deficiency, and eventually the buoyant forces will become dominant, turning the buoyant jet into a plume. Both flows, turbulent jets and plumes, are an effective mechanism to accomplish high levels of initial dilution because they entrain large volumes of ambient fluid and mix it with the discharged fluid. Since all discharges go through one or both of these phases, it is important to develop some knowledge on pure jets, buoyant jets, and pure plumes in order to understand and be able to predict the fate of pollutants discharged from a marine outfall.

Apart from the effects induced by the geometry of the discharge port, the dynamics of a turbulent jet depend on the values of its mass flux, momentum flux, and buoyancy flux at the source, their relative magnitude, and how they evolve with time. In a real waterbody, the jet behaviour will also depend on environmental parameters such as local turbulence levels, possible density stratification, and the presence of currents. The three fluxes mentioned above, as defined in Fischer *et al.* (1979), are calculated as:

a) the mass flux of the jet, given by

$$\rho q = \int_A \rho w dA \tag{4.1}$$

which is the mass of fluid passing a jet cross-section of area A per unit time. In the above equation, w is the time-averaged jet velocity in the axial direction, and q is the volume flux of the jet.

b) the momentum flux of the jet, which is the amount of streamwise momentum passing a jet cross-section per unit time:

$$\rho m = \int_A \rho w^2 dA \tag{4.2}$$

c) the buoyancy flux, the buoyant weight of the fluid passing through a jet cross-section per unit time. If $\Delta\rho$ is the difference in density between the ambient fluid and the fluid of the jet, this variable may be expressed as

$$\rho\beta = \int_A g\Delta\rho w dA \tag{4.3}$$

The value of these parameters at the source, divided by the density ρ, will be denoted throughout this chapter by Q, M, and B, respectively.

4.1.1 The pure jet

A jet is defined as the discharge of a fluid from an orifice into a large body of the same of similar fluid (Fischer *et al.*, 1979), driven by the momentum of the source.

The boundaries between the ambient and jet fluids are very fluctuating, but they are quite sharp at any instant; however, both the time-averaged velocity and tracer concentration distributions are essentially Gaussian (Fischer *et al.*, 1979), in the form

$$F = F_m \exp\left[-K\frac{x^2}{z^2}\right] \tag{4.4}$$

where F_m is the value of F on the jet axis, z is the distance along the jet axis, and x is the radial distance from the axis.

For the velocity, this equation holds true only at a distance greater than about six jet diameters, or seven port diameters, downstream (Wood *et al.*, 1993), since within this distance the original velocity has not yet been changed from the pipe velocity distribution to the velocity distribution determined by the jetlike flow ("zone of flow establishment"-ZFE-; Fischer *et al.*, 1979). In fact, the same authors point out that the equilibrium of the turbulent flow within the jet is not reached until approximately ten diameters downstream, when the turbulence attains a state of steady decay. Outside this region, the flow is long in the direction of the mean velocity, and narrow in the perpendicular direction, implying that changes in the direction of the flow are an order of magnitude smaller than changes perpendicular to the flow, and the flow is approximately in local equilibrium with all the local properties that depend only on local mean parameters.

Downstream of the ZFE, in the so-called "zone of established flow", the velocity and concentration profiles become self-similar, i.e., that at any cross-section of the jet the time-averaged velocity, tracer concentration or buoyancy can be expressed as a function of a maximum (centreline) value, and a measure of the width. The most usual function is Gaussian, so that

$$w = w_m \exp(-x^2/b_w^2) \tag{4.5}$$

$$C = C_m \exp(-x^2/\lambda^2 b_C^2) \tag{4.6}$$

$$B = B_m \exp(-x^2/\lambda^2 b_B^2) \tag{4.7}$$

in which b_w, b_C and b_B are the distance from the source at which the centreline values of w, C and B are reduced by a factor $1/e$, and λ is a parameter that accounts for the difference in the spread of velocity and concentration, with approximate values of 1.275 for jets, and 1.067 for plumes (Wood *et al.*, 1993).

By applying dimensional analysis, the dependence of w_m, C_m, b_w and b_c on the distance to the jet source can be determined. Fischer *et al.* (1979) have shown that, for distances larger than a given lengthscale l_Q ($=Q/M^{1/2}$, a measure of the distance at which the geometry of the discharge port still influences the flow), all properties of the jet are defined solely in terms of the distance z to the source and the initial momentum flux, M. In particular, the centreline velocity w_m is found to be

$$w_m = a_1 \frac{M}{Q}\left(\frac{l_Q}{z}\right) \qquad \text{for } z >> l_Q \tag{4.8}$$

where a_1 is an experimental constant. This equation fits well with the experimental data obtained by five different researchers, as shown in figure 4.1, provided that a_1 takes the value 7.0:

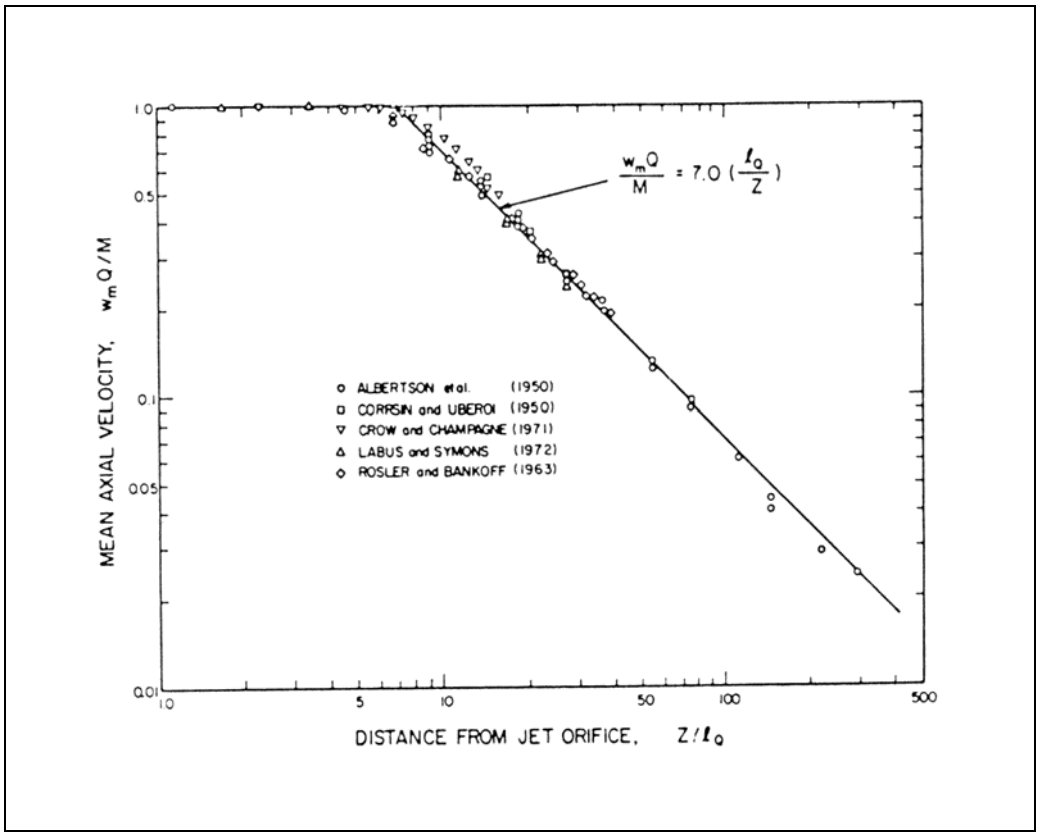

Figure 4.1: Decay of the mean centreline velocity, for a round buoyant jet. From Fischer *et al.* (1979).

A similar reasoning yields an analogous expression for the tracer mass concentration C_m:

$$C_m = a_2 C_0 \left(\frac{l_Q}{z} \right) \tag{4.9}$$

where C_0 is the initial concentration, and a_2 is another empirical constant, whose value depends on the geometry of the jet. For round jets, Chen and Rodi (1976) –cited in Fischer *et al.* (1979)- suggested a_2 = 5.64.

Wood *et al*. (1993) also proposed expressions for the centreline velocity and tracer concentration, and included an estimation of the jet radius *b*:

$$w_m = K_{jw} w_0 \left(\frac{\pi}{4} \right)^{1/2} \left(\frac{z}{d_p} \right)^{-1} \tag{4.10}$$

$$b = K_{jb} z \tag{4.11}$$

$$C_m = K_{jc} C_0 \left(\frac{\pi}{4}\right)^{1/2} \left(\frac{z}{d_p}\right)^{-1} \tag{4.12}$$

where w_0 is the initial velocity, d_p is the initial jet diameter, and the values for the constants K_{jw}, K_{jb}, K_{jc} have been determined experimentally as 7.57, 0.11, and 6.06, respectively (Papanicolaou, 1984).

4.1.2 The pure plume

In opposition to jets, a plume is defined as a source of buoyancy flux only, with no initial momentum or volume fluxes (Roberts, 1979). Since there is no initial momentum flux, all flow variables must be a function only of the initial buoyancy flux B, the viscosity of the fluid ν, and the distance z to the source. Again using dimensional analysis, and assuming a completely turbulent flow in which any viscosity effects are negligible, the decay of the plume centreline velocity can be estimated as

$$w_m = b_1 \left(\frac{B}{z}\right)^{1/3} \tag{4.13}$$

where the value of b_1 is given as 4.7 (Fischer *et al.*, 1979; Rouse *et al.*,1952).

Similarly, expressions can be derived to describe the changes in centreline tracer concentration and momentum flux. This latter variable was approximately constant for the pure jet, but now increases along the plume axis as a consequence of the density difference between the fluid within the plume and its surroundings.

$$C_m = b_2 C_0 \left(\frac{1}{Bz^5}\right)^{1/3} \tag{4.14}$$

$$m = b_3 B^{2/3} z^{4/3} \tag{4.15}$$

with b_2 = 9.1 (Chen and Rodi, 1976), and b_3 = 0.35, for a round plume (Fischer *et al.*, 1979).

Again, Wood *et al*. (1993) give somewhat different expressions for the centreline velocity and concentration, and for the plume width, for the case of a pure axisymmetric plume, although the dependence on z remains unchanged:

$$w_m = K_{pw} w_0 \left(\frac{\pi}{4}\right)^{1/3} Fr_0^{-2/3} \left(\frac{d_p}{z}\right)^{1/3} \tag{4.16}$$

$$b = K_{pb} z \tag{4.17}$$

$$C_m = K_{pc} C_0 \left(\frac{\pi}{4}\right)^{2/3} Fr_0^{2/3} \left(\frac{d_p}{z}\right)^{5/3} \tag{4.18}$$

where the values for K_{pw}, K_{pb}, and K_{pc} are respectively 3.85, 0.105 and 11.1 (Papanicolaou, 1984). Here, the densimetric Froude number Fr_0 has been introduced, as the rate of the buoyancy and the momentum forces:

$$Fr_0 = \frac{w_0}{\sqrt{g'_0 d_p}} \tag{4.19}$$

with g'_0 the initial effective gravity: $$g'_0 = g\frac{\Delta\rho}{\rho_r} \tag{4.20}$$

where ρ_r is a reference density.

4.1.3 The buoyant jet

The most common flow resulting from a marine discharge is that of a buoyant jet, defined as a jet whose initial density differs from the density of the receiving water by an amount $\Delta\rho_o$. Any buoyant jet will behave in a jetlike manner or in a plumelike manner depending on its initial volume flux, momentum flux, and buoyancy flux, but in the long run, and given enough space, all buoyant jets will turn into plumes.

A measure of the distance from the source at which the behaviour of a jet becomes plumelike in a stagnant environment is given by the lengthscale l_M, defined as

$$l_M = \frac{M^{3/4}}{B^{1/2}} \tag{4.21}$$

The type of flow is determined by the ratio z/l_M: if z/l_M is small (<<1), the flow will behave like a jet, and the equations given in §4.1.1 are valid; in the opposite case, the flow is plumelike, and the equations from §4.1.2 can be applied. In general, the initial region of the flow is dominated by the initial momentum, and behaves asymptotically as described for a pure jet; the final almost vertical plume phase is dominated by the buoyancy-generated momentum, and behaves asymptotically as described for the vertical plume. This fact is illustrated in figure 4.2, in which the dimensionless mean dilution (here denoted $\overline{\mu}$) and distance to the source (ζ) are obtained using the equations for round jets given in Fischer *et al.* (1979):

$$\overline{\mu} = \frac{q}{Q}\left(\frac{R_0}{R_p}\right) \tag{4.22}$$

$$\zeta = c_p\left(\frac{z}{l_Q}\right)\left(\frac{R_0}{R_p}\right) \tag{4.23}$$

The variable R_0 is called the jet Richardson number, and is defined as the ratio of l_Q and l_M:

$$R_0 = \frac{l_Q}{l_M} = \frac{QB^{1/2}}{M^{5/4}} \overset{\text{round jet}}{=} \left(\frac{\pi}{4}\right)^{1/4}\left(\frac{g'_0 d_p}{w_0^{\,2}}\right)^{1/2} = \left(\frac{\pi}{4}\right)^{1/4}\frac{1}{Fr_0} \tag{4.24}$$

whereas R_p is the so-called plume Richardson number, or

$$R_p = \frac{qB^{1/2}}{m^{5/4}} \tag{4.25}$$

and c_p is the growth coefficient for plumes, $c_p = b_w\sqrt{2\pi}/z$. (4.26)

In case the buoyant jet is discharged at an angle to the vertical, the Richardson number must implicitly include a specification of the jet orientation. Fischer *et al.* (1979) point out that a horizontal buoyant jet rises exponentially with distance from the source, and that the scaling length is again l_M.

For a general analysis, the elevation angle θ_V at which the effluent is discharged relative to the horizontal plane must be introduced in the calculations, making it impossible to obtain complete solutions for the buoyant jet from simple dimensional analysis (Wood *et al.*, 1993), and a set of equations must be used. These involve the horizontal and vertical momentum, geometric considerations (4.27c,d) and a closure condition:

$$\frac{dm_{t*}}{ds_*} = \left(\frac{4}{\pi}\right)^{0.5}\left(\frac{I_{g'}I_m^{0.5}}{I_\beta}\right)\frac{b_*}{Fr_0^{\,2}}\frac{\left[m_{t*}^2 - m_{H*}^2\right]^{0.5}}{m_{t*}^{1.5}} \tag{4.27a}$$

$$\frac{dx_*}{ds_*} = \frac{m_{H*}^2}{m_{t*}^2} \tag{4.27b}$$

$$\frac{dz_*}{ds_*} = \frac{\left[m_{t*}^2 - m_{H*}^2\right]^{0.5}}{m_{t*}} \tag{4.27c}$$

$$\frac{db_*}{ds_*} = k_s \tag{4.27d}$$

In the above set of equations, m_{H*}, m_{V*}, and m_{t*} are the normalised horizontal, vertical, and total momentum, k_s is a spread coefficient, the variables with subscript * are the dimensional variables divided by d_p (e.g., $x_* = x/d_p$), the vertical coordinate is z ($=z_*\cdot d_P$), and s ($=s_*\cdot d_p$) is the distance to the source. The parameters I_β, I_m, and $I_{g'}$ are shape constants defined in eq. (4.28.c-e):

$$m_{V*} = I_m w_m^2 b^2 \sin\theta_V / m \tag{4.28a}$$

$$m_{H*} = I_m w_m^2 b^2 \cos\theta_V / m \tag{4.28b}$$

$$I_m = \int_0^\infty \left[\frac{w}{w_m}\right]^2 2\pi\varsigma d\varsigma = \frac{\pi}{2} \tag{4.28c}$$

$$I_{g'} = \int_0^\infty \frac{g_L'}{g_m'} 2\pi\varsigma d\varsigma = 3.5767 \tag{4.28d}$$

$$I_\beta = \int_0^\infty \left(\frac{g_L'}{g_m'}\frac{w}{w_m} + \frac{\overline{w'g_L''}}{\overline{wg_L'}}\right) 2\pi\varsigma d\varsigma = 1.9903 \tag{4.28e}$$

with $\varsigma = r/b$, where r is the distance to the jet axis, and where g_L' and g_m' are the local and centreline effective gravity, and w' and g_L'' are turbulent fluctuations of w and g_L'.

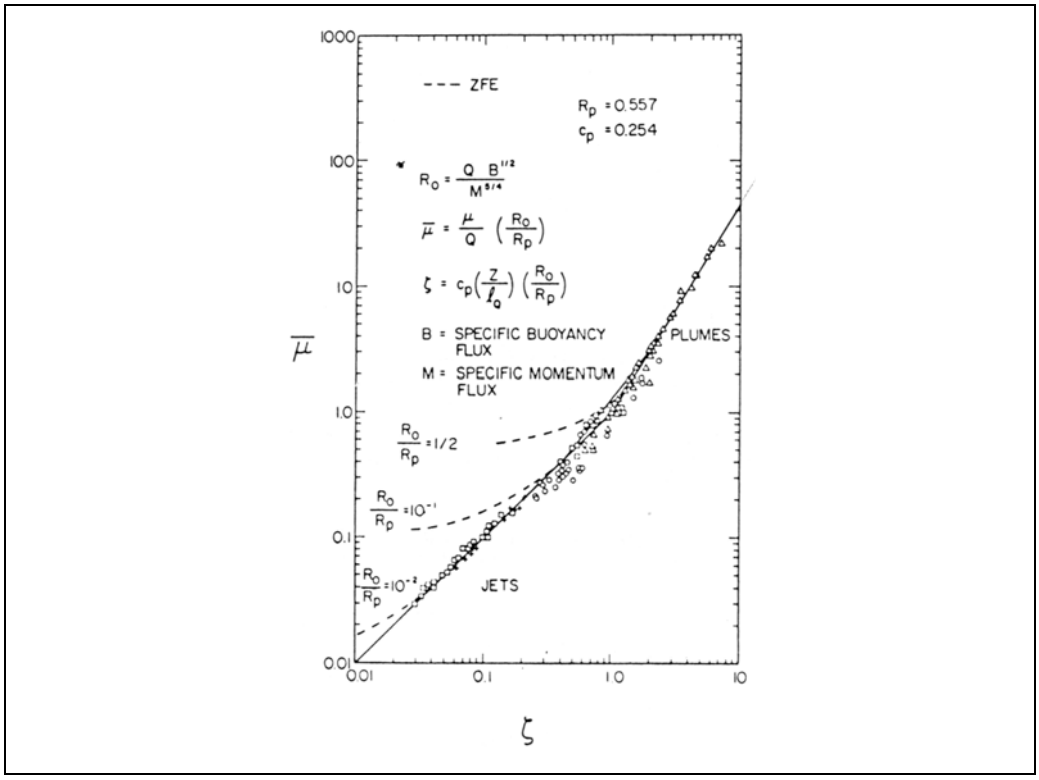

Figure 4.2: Asymptotic solutions for dilution in a vertical round jet, compared to data from experiments. Here, R_0 is a Richardson number, $\overline{\mu}$ and ζ are dimensionless mean dilution and distance from the source, respectively (from Fischer *et al.*, 1979).

The dilution for vertical plumes -Wood *et al.* (1993)- and horizontal buoyant jets -Cederwall (1968)- can be calculated as follows:

$$S = 0.117 Fr_0^{-0.66}\left(\frac{z}{d_p}\right)^{1.66} \qquad \text{-vertical plume-} \qquad (4.29)$$

$$\frac{S}{Fr_0} = \begin{cases} 0.54\left(\dfrac{0.38}{Fr_0}\dfrac{z}{d_p} + 0.66\right)^{1.66} & \dfrac{z}{d_p} > 0.5 Fr_0 \\ \left(\dfrac{z}{d_p Fr_0}\right)^{7/16} & \dfrac{z}{d_p} < 0.5 Fr_0 \end{cases} \qquad \text{-horizontal buoyant jet-} \qquad (4.30)$$

Additionally, an expression for the dilution of a buoyant jet was proposed by Roberts (1987), in the form

$$S = 0.118\left(\frac{z}{l_M}\right)^{5/3} Fr_0 \qquad (4.31)$$

The agreement between these formulae and measured data is good, as can be seen in figures 4.3a-b.

4.1.4 The merging of jets and plumes

Submarine outfalls in shallow coastal waters are often designed with a port spacing comparable to, or greater than, the water depth in order to avoid interference between adjacent wastewater plumes before the surface or the terminal height of rise is reached (Lee and Cheung, 1990). However, for a marine outfall consisting of an array of ports spaced at a distance p_s along a horizontal axis, the most probable result will be the merging of the individual plumes at some height above the outfall axis, even if the discharge from each port occurs in different directions. The flow field in the central part of the diffuser length may then be considered as a two-dimensional -or plane- buoyant jet; at either end of the pipe, the flow becomes extremely complicated, and this approximation is no longer acceptable. The 2D buoyant jet assumption is best for fairly low discharge rates, large density differences, deep waters, and closely spaced jets. Figure 4.4 (from Wood *et al.*, 1993) illustrates the merging of vertical jets in a stagnant environment.

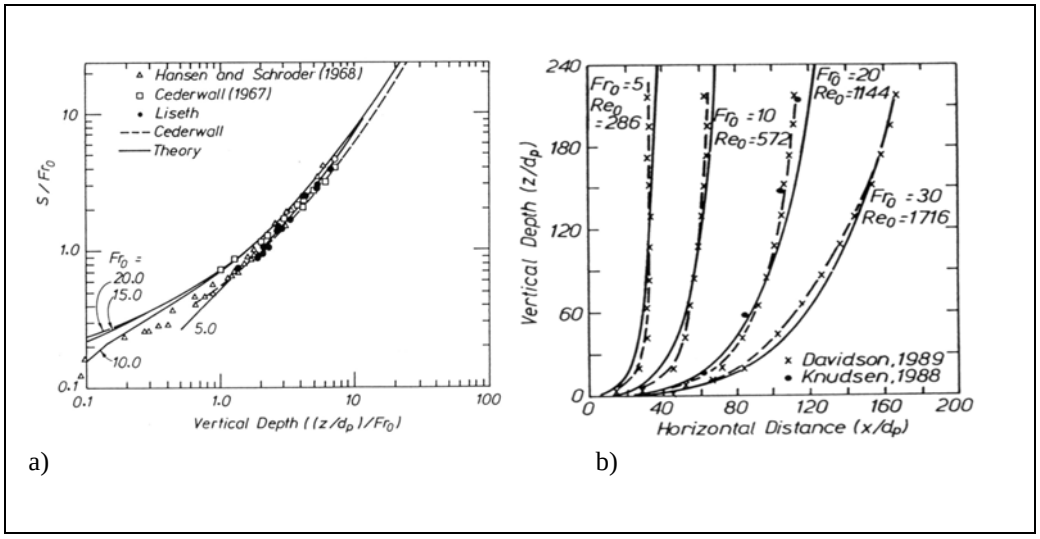

Figure 4.3: Comparison of measurements with computed solutions. **a)** Dilution, using Cederwall's empirical formula (4.30). **b)** Plume trajectories, calculated using a numerical model based on equations (4.27). From Wood *et al.* (1993).

In the qualitative model presented by Wood *et al.* (1993) to describe the flow in the merging region above the outfall three main different phases are considered. In the first phase, below the level M_1 in figure 4.5, the buoyant jets arising from each port are considered axisymmetric and treated individually; at M_1, the buoyant jets on the same side of the outfall merge, and the resulting flows on each side back towards the outfall centreline until, at section 3, they merge, although conserving their individual properties. At section 4 the merged plume becomes a single two-dimensional plume.

Below M_1, the entrainment is due to the local elevation. Through the inner surface from M_1 to M_2, however, the entrainment must come from an elevation below the position where the axisymmetric plumes merge (M_1). This is illustrated in sections *CC* and *DD* (figure 4.5e,f). The streamline EM_1 divides the flow that is entrained locally and the flow that is entrained on the inner

surface M_1M_2. This flow is best discussed using the entrainment concept. Until the entrained flow enters the turbulent jet it is in an irrotational flow region. Thus, if Bernouilli's equation is used for the streamline from the region far from the diffuser where the flow is almost axisymmetric, the pressure at *B* is the same as that outside. This contrasts with the streamline coming from outside the flow to point *C* in section *CC*. This point is in a region of the upflow required to satisfy the entrainment demand of the inner surface M_1M_2 and the application of the Bernouilli equation to this streamline gives a pressure below the hydrostatic pressure outside, i.e., an underpressure. A similar statement can be made about the point *D* in section *DD*, and it is the distribution of this underpressure (figure 4.5c) that forces the buoyant jets to merge.

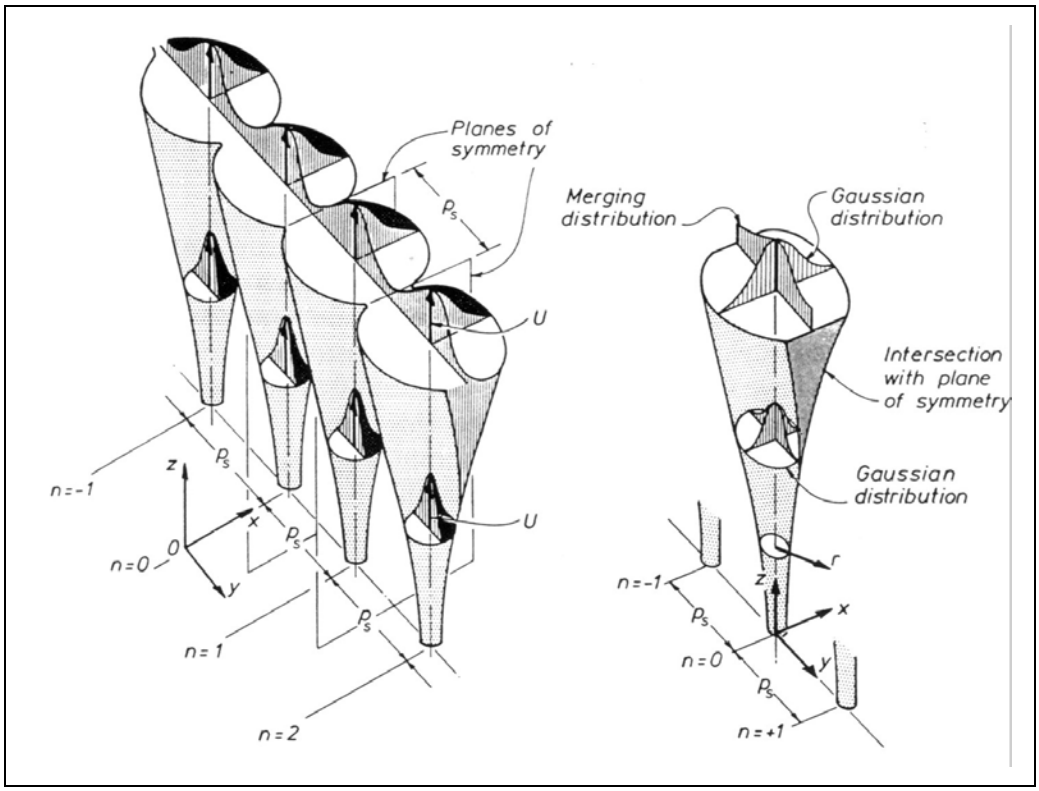

Figure 4.4: The merging of axisymmetric buoyant plumes (from Wood *et al.*, 1993).

From the point M_2 there must be a positive pressure on the centreline plane until the horizontal momentum component of the merging buoyant jets is reduced to zero and the flow is vertical. The vertical momentum of the flow approaching M_2 must also change, and the forces necessary for this change require a pool of lighter effluent at M_2. The angle at which the two-dimensional plume meets is small and thus this change and the reduction in the entrainment caused by the pool of lighter fluid will always be small.

In the region from *E* to M_2, the underpressure should change the rate of generation of both the horizontal and the vertical momentum in the plume. However, the change in the vertical momentum will be dominated by the buoyancy forces, which are an order of magnitude greater than any forces due to the pressure gradient. On the other hand, the only force changing the horizontal momentum is that due to the pressure gradient, and this force must be included in the equations.

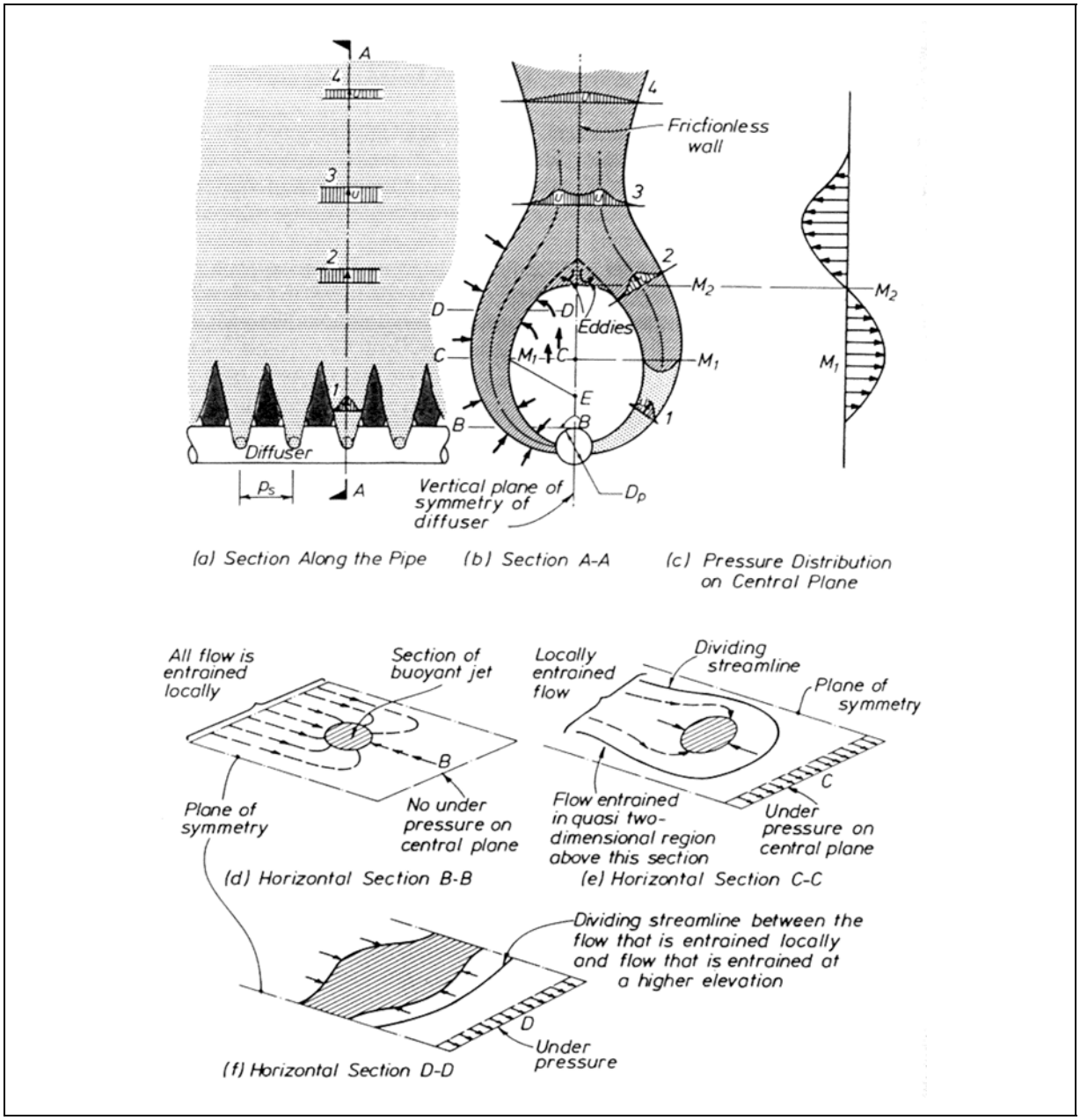

Figure 4.5: Schematic diagram for the model of merging buoyant jets (from Wood *et al.*, 1993).

Wood *et al.* (1993) argue that, since the velocity distribution for axisymmetric and plane buoyant jets are given by

$$\frac{w}{w_m} = \exp\left\{-\frac{r^2}{b_w^2}\right\} \tag{4.32}$$

$$\frac{w}{w_m} = \exp\left\{-\frac{x^2}{b_w^2}\right\} \tag{4.33}$$

respectively, a reasonable distribution for the velocity in the transition region between both types of jets can be found by combining (4.32) and (4.33):

$$w = w_m \frac{\exp\left(-x_b^2\right)\sum_{n=-\infty}^{\infty} \exp\left\{-\left(\frac{y_p+n}{b_p}\right)^2\right\}}{\sum_{n=-\infty}^{\infty} \exp\left\{-\left(\frac{n}{b_p}\right)^2\right\}} \tag{4.34}$$

where $x_b = x/b_w$, $y_p = y/p_s$, and $b_p = b_w/p_s$. For the tracer concentration distribution, a similar equation is used, replacing b_w/p_s with $\lambda b_C/p_s$:

$$C = C_m \frac{\sum_{n=-\infty}^{\infty} \exp\left\{-\left(\frac{(y_p+n)^2+x_b^2}{\lambda^2 b_p^2}\right)\right\}}{\sum_{n=-\infty}^{\infty} \exp\left\{-\left(\frac{n}{\lambda b_p}\right)^2\right\}} \tag{4.35}$$

It can be seen that these distributions are equivalent to the axisymmetric profile near the source (b_w/p_s, $\lambda b_C/p_s$ <<1), satisfy the two-dimensional distribution for b_w/p_s, $\lambda b_C/p_s$ >>1, and move smoothly between both limiting cases. Wang and Davidson (1999) remark that the above distributions are obtained by assuming that both the velocity and concentration distributions of the merging jets are additive, although the velocity and concentration distributions within a jet cross-section should be based on the summation of the quantities that are conserved, i.e., the momentum and the tracer fluxes. They develop a jet merging model that shows that equations (4.34) and (4.35) are correct for weak jets (whose behaviour is strongly affected by the ambient flow), but must be corrected when the jet behaviour is dominated by the jet excess momentum (strong jets), yielding

$$w = w_m \frac{\exp\left(-2x_b^2\right)\sum_{n=-\infty}^{\infty} \exp\left\{-2\left(\frac{y_p+n}{b_p}\right)^2\right\}}{\sum_{n=-\infty}^{\infty} \exp\left\{-2\left(\frac{n}{b_p}\right)^2\right\}} \tag{4.36}$$

$$C = C_m \frac{w_m}{w} \frac{\sum_{n=-\infty}^{\infty} \exp\left\{-\left(\frac{(y_p+n)^2+x_b^2}{b_p^2}\right)\left(\frac{1+\lambda^2}{\lambda^2}\right)\right\}}{\sum_{n=-\infty}^{\infty} \exp\left\{-2\left(\frac{n}{b_p}\right)^2\left(\frac{1+\lambda^2}{\lambda^2}\right)\right\}} \tag{4.37}$$

The shape “constants” given in §4.1.3 are also valid for merging buoyant jets, but they can no longer be considered to have constant values. The selected shape functions (I'_m, I'_β, $I'_{g'}$, and I'_q, to

differentiate them from the constant values) vary smoothly from their axisymmetric values to their two-dimensional plume values, as complex functions of b_w/p_s and $\lambda b_C/p_s$. Their analytical expressions can be found in Wood *et al*. (1993), together with a complete analysis of the equations of momentum and trajectory equations for merging plumes, considering first the region below the point at which the two two-dimensional buoyant jets merge, and then the region above. A comparison of their equations with experimental data shows that although the agreement is satisfactory before the plume merging, after this point the computed dilution is about 20% higher than the observed values.

The same experimental data was used by Roberts (1987) to give an estimation of the dilution above a row of merging buoyant jets as

$$\frac{S_m}{Fr_0} = 0.50\left(\frac{2z}{p_s}\right)^{-2/3}\left(\frac{z}{d_p Fr_0}\right)^{5/3} \qquad (4.38)$$

when $2z/p_s > 50$.

4.2 THE EFFECT OF ENVIRONMENTAL FACTORS ON DISPERSION

Although the discharge parameters, such as the characteristics of the ports and the orientation of the jet, play an important role in the process of initial jet dilution, a series of factors exist that can not be predicted by the engineer, and which govern the evolution of the discharge after the initial dilution phase, including both the shape of the resulting plume and the concentration distribution.

To illustrate this fact, Petrenko *et al.* (1998) point out a series of environmental processes which explain the complexity of plume shapes:

a) the plume shape appears to be more complex when current and stratification conditions result in a Froude number (Fr_0) larger than 10 (Roberts *et al.*, 1989). It also depends on the angle between the current and the plume discharge,

b) plume shapes also vary on timescales of minutes to hours due to temporal variations of Fr_0, i.e., rapid variations in currents and stratification, which may lead to changes in the equilibrium depth, creating gaps between various plume layers,

c) internal tides may also contribute to the plume's spatial complexity, since it has been found that the equilibrium depth of plumes follows the vertical displacements of isopycnal surfaces, which can be driven by semidiurnal internal tides,

d) several plumes may also appear in response to variations in current shear; this may happen if discharges occur over a wide depth range with distinct temperature, salinity and current gradients.

As is clear from the list above, the environmental factors that affect the behaviour of an outfall discharge are, mainly, density stratification and ambient currents.

4.2.1 Density stratification

Stratification of the water column is a frequent phenomenon in coastal regions, and is associated with variations in salinity and temperature.

In a stably stratified environment, the jet first behaves like a buoyant jet and mixes with the heavy bottom fluid as it rises, producing a neutrally buoyant cloud. During the rise, the buoyant force is provided by the density difference between the rising effluent and the density of the surrounding fluid at the level of the effluent. The initial density deficit of the buoyant jet will continuously decrease and become zero at a certain height z_e above the discharge point, perhaps below the surface. The buoyancy force will be negative from here on, and the flow will be decelerated and turned down after reaching a maximum height z_t, depending on the momentum flux at the equilibrium level. Therefore, the major effects of density stratification are to limit the vertical rise of the effluent, and to restrict the mixing of the jet flow with the surrounding fluid (Hwang *et al.*, 1995), although Anwar (1998) presents data which reveals that plume lateral and vertical spread is also influenced by water stratification.

In particular, Anwar (1998) found that, in uniform coastal waters, the plume spread in the lateral and vertical directions, estimated from the plume variance σ^2, was well approximated by the expression

$$\sigma^2 = A_1 t^{b_1} \tag{4.39}$$

where A_1 is a dimensional constant. For lateral spread, A_1=0.43 and b_1=1.63, whereas A_1=0.48 and b_1=0.78 for the vertical spread. On the other hand, if the coastal waters presented stratification, the plume became quickly mixed over the top layer of the water column, and the horizontal spread was well described by (4.39) with A_1=0.09 and b_1=2.10.

Experiments by Abraham and Eysink, cited in Wood *et al.* (1993), show that, above the equilibrium point, the plume density on the centreline is approximately constant, as it can be seen in figure 4.6. In this region of upflow above the equilibrium level the measurement of density deficit showed that while the centreline density deficit may have been constant, the density deficit distribution and, hence, the buoyancy distribution, continued to spread.

Consider a point source of momentum directed vertically upward. The effect of this momentum flux will be to carry entrained dense fluid to where the ambient fluid is less dense; therefore, there will exist a terminal height of rise, z_t, which must be a function of a density field characteristic (e.g., the gradient of the density profile) and the initial momentum flux M. An analogue argument can be used for point sources of buoyancy flux B (plumes). If the density profile is linear, Fischer *et al.* (1979) give the following expressions for the terminal height of rise for a round simple jet and a round simple plume, respectively:

$$z_t \propto \left(\frac{M}{N} \right)^{1/4} \tag{4.40}$$

$$z_t \propto \left(\frac{B}{(N)^{3/2}} \right)^{1/4} \tag{4.41}$$

where N is

$$N = -\frac{g}{\rho_0}\frac{d\rho_a}{dz} \tag{4.42}$$

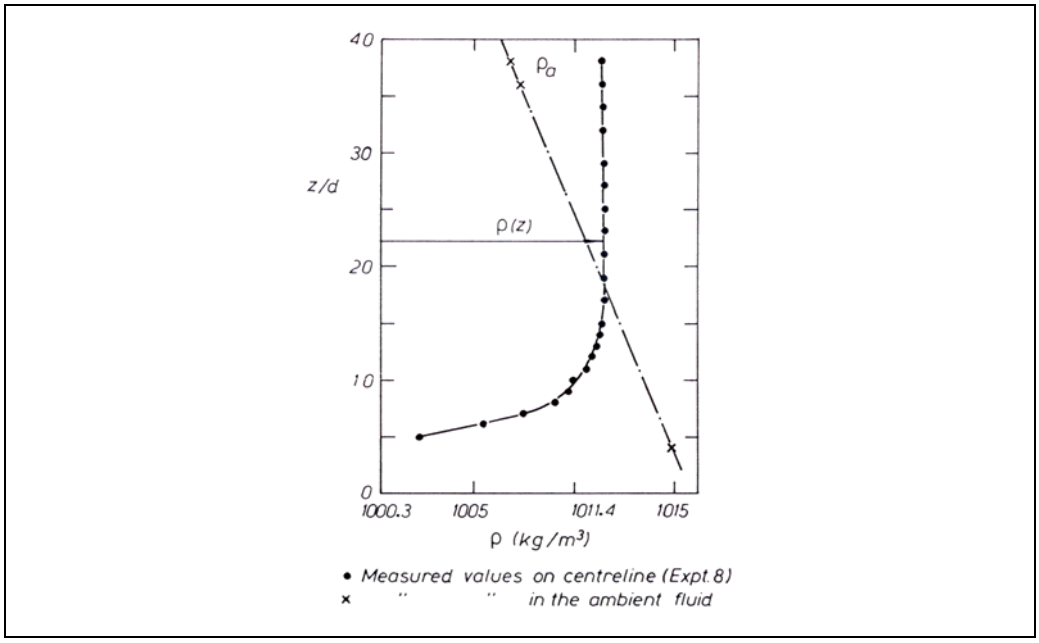

Figure 4.6: The density distribution on the plume centreline (after Abraham and Eysink, 1969).

and the coefficient of proportionality is approximately 3.8. The terms on the right-hand side define characteristic lengthscales for jets and plumes in density stratified environments with a constant density gradient, and their ratio J can then be used to obtain an asymptotic functional relationship for the terminal height of rise for buoyant plumes:

$$J = \frac{M^2 N}{B^2} \tag{4.43}$$

$$z_t \rightarrow \begin{cases} a_p J^{-3/8} & J \ll 1 \\ a_j J^{-1/4} & J \gg 1 \end{cases} \tag{4.44}$$

with a_p and a_j equal to 1.7 ± 0.2, according to Fischer *et al.* (1979).

The mean dilution at z_t must also be given by asymptotic results (Fischer *et al.*, 1979):

$$S_m \rightarrow \begin{cases} e_p J^{-5/8} & J \ll 1 \\ e_j J^{-1/4} & J \gg 1 \end{cases} \tag{4.45}$$

with $e_p = 1.5 \pm 0.2$ and $e_j = 1.2 \pm 0.2$.

Roberts (1987) defined a new lengthscale l'_B, which is proportional to the maximum height of rise of a point plume in a linearly stratified stagnant fluid, as

$$l'_B = \frac{B^{1/4}}{N^{3/8}} \tag{4.46}$$

and, by using dimensional analysis, and neglecting the effect of source volume flux, he found that the main wastefield parameters, i.e.

$$\frac{S_m Q N^{5/4}}{B^{3/4}} \quad \frac{z_t}{l'_B} \quad \frac{z_e}{l'_B} \quad \frac{h_e}{l'_B} \tag{4.47}$$

were all functions of l_M/l'_B, and their solutions for arbitrary conditions had to be obtained from numerical models. However, Wong (1985) found that, for vertical buoyant jets with $l_M/l_B < 0.6$,

$$\frac{S_m Q N^{5/4}}{B^{3/4}} = 0.80 \tag{4.48}$$

$$\frac{z_t}{l'_B} = 4.5 \tag{4.49}$$

$$\frac{z_e}{l'_B} = 1.5 \tag{4.50}$$

$$\frac{h_e}{l'_B} = 2.9 \tag{4.51}$$

On the other hand Wood *et al.* (1993), also based on dimensional analysis, find that the maximum height of rise of an axisymmetric buoyant jet is given by

$$z_t = \frac{M^{3/4}}{\beta^{1/2}}\left[C_1\left(\frac{\beta}{N^{1/2}M}\right)^{1/2} + C_2\left(\frac{\beta}{N^{1/2}M}\right)^{3/4}\right] \tag{4.52}$$

whereas for a two-dimensional plume, z_t can be obtained as

$$z_t = \frac{M}{\beta^{2/3}}\left[C_5\left(\frac{\beta}{N^{1/2}M}\right)^{2/3} + C_6\left(\frac{\beta}{N^{1/2}M}\right)\right] \tag{4.53}$$

where C_1, C_2, C_5, and C_6 are experimental constants. The dilution for both types of discharges is found to be, respectively,

$$S = \frac{M^{5/4}}{Q\beta^{1/2}}\left[C_3\left(\frac{\beta}{N^{1/2}M}\right)^{1/2} + C_4\left(\frac{\beta}{N^{1/2}M}\right)^{5/4}\right] \tag{4.54}$$

and

$$S = \frac{M}{Q\beta^{1/3}}\left[C_7\left(\frac{\beta}{N^{1/2}M}\right)^{1/3} + C_6\left(\frac{\beta}{N^{1/2}M}\right)\right] \tag{4.55}$$

where again the C_i are experimental constants. The derivation of equations (4.52) to (4.55) has been done assuming a linear density profile; as shown in figures 4.7 and 4.8, both the maximum rise height and the maximum dilution obtained from these equations are compatible with measured values. Experimental data suggests that the thickness of the spreading layer is about 40% of the maximum height of rise, but measurements by Wright and Wallace (1984) show that this parameter depends on whether the flow is momentum dominated, or buoyancy dominated (fig. 4.9).

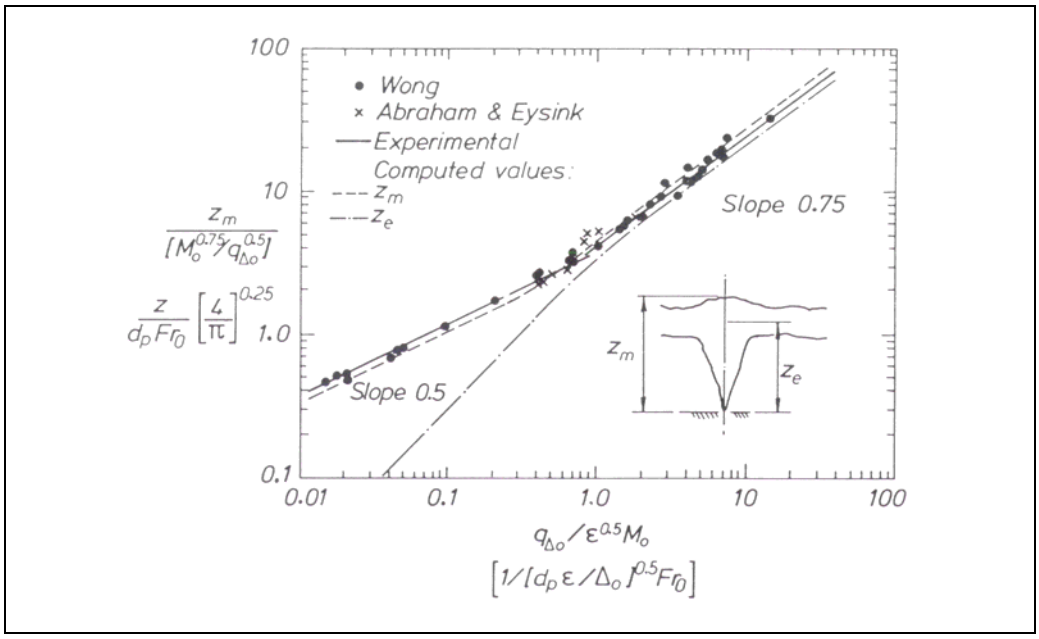

Figure 4.7: Dimensionless maximum rise height of a vertical axisymmetric plume in a linearly stratified fluid (from Wood *et al.*, 1993).

Finally, Morton *et al.* (1956) and Brooks (1972) also yield expressions for the terminal height of rise and the centreline dilution at z_t in a linearly stratified environment:

$$z_t = 3.98 l'_B \tag{4.56}$$

$$S_m = 0.071\frac{B^{1/3}}{Q} z_t^{5/3} \tag{4.57}$$

When the density profile is not linear, or the buoyant jet is discharged at a certain angle to the vertical, the above approach does not provide a suitable basis for wastefield estimation, and more detailed numerical models, which consider the flow below and above the equilibrium region, must be brought in.

Below the equilibrium region, Wood *et al.* (1993) suggest the following equation for the flux of density difference,

$$\frac{d}{ds}\int_0^{b'}\rho_L w 2\pi r dr = Q_i \rho_a(z) \tag{4.58}$$

where ρ_L is the local density, $\rho_a(z)$ is the ambient density at level z, and Q_i is the volumetric inflow per unit of trajectory length into the buoyant jet. After manipulation, this equation becomes

$$\frac{d}{ds}\int_0^{b'} w g_L' 2\pi r dr = -\sin\theta \frac{dg_a'(z)}{dz}\int_0^{b'} w 2\pi r dr \tag{4.59}$$

where

$$g_L' = \left[\frac{\rho_a(z)-\rho_L}{\rho_a(0)}\right] g \tag{4.60}$$

$$g_a' = \left[\frac{\rho_a(0)-\rho_a(z)}{\rho_a(0)}\right] g \tag{4.61}$$

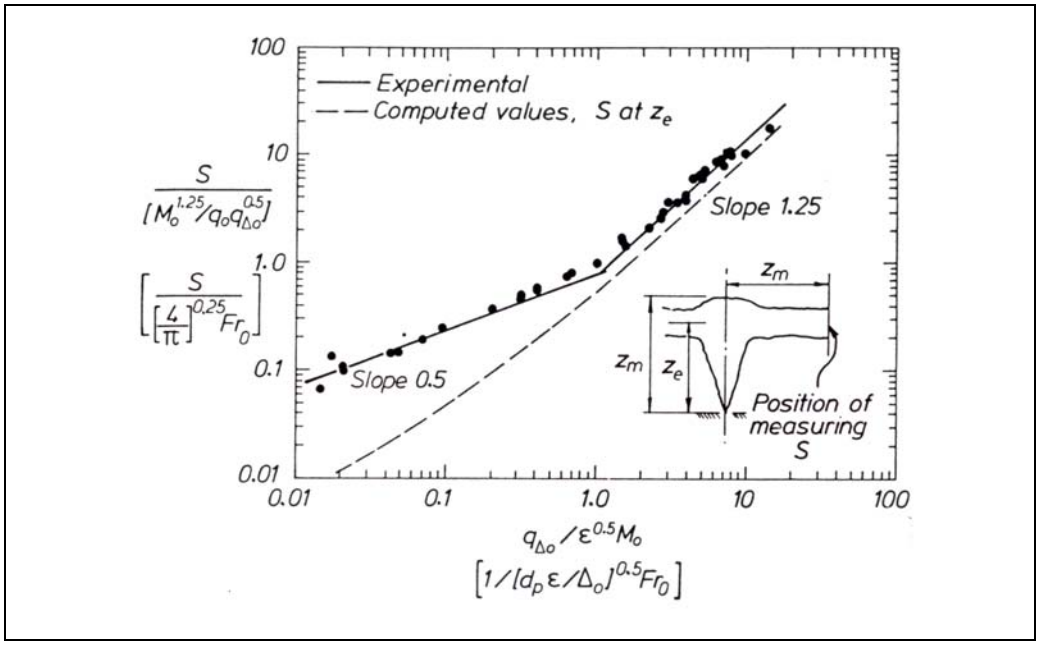

Figure 4.8: Dimensionless maximum dilution in the spreading layer from a vertical axisymmetric plume in a linearly stratified fluid (from Wood *et al.*, 1993).

The new dimensionless vertical momentum and flux of density difference equations become

$$\frac{dm_{V*}}{ds_*} = \left(\frac{4}{\pi}\right)^{1/2} \frac{I'_{g'}(I'_m)^{1/2}}{I'_\beta Fr_0^{\,2}} \frac{(p_{s*}b_*)}{m_{t*}^{\,2}} \beta_* \tag{4.62}$$

where

$$\beta_* = \beta / B \tag{4.63}$$

and
$$\frac{d\beta_*}{ds_*} = \left(\frac{4}{\pi}\right)^{1/2} \frac{I'_q}{(I'_m)^{1/2}} (b_* p_{s*})^{1/2} \frac{m_{V*}}{m_{t*}^{1/2}} \frac{dg_a'_*}{dz_*} \tag{4.64}$$

with
$$g_a'_* = g_a' / g_0' \tag{4.65}$$

The remaining equations are the spread equation (4.27d), two geometry equations (4.27b-c) and the horizontal momentum equation (4.27a). This set of equations governs the behaviour of the plume before it reaches the equilibrium region.

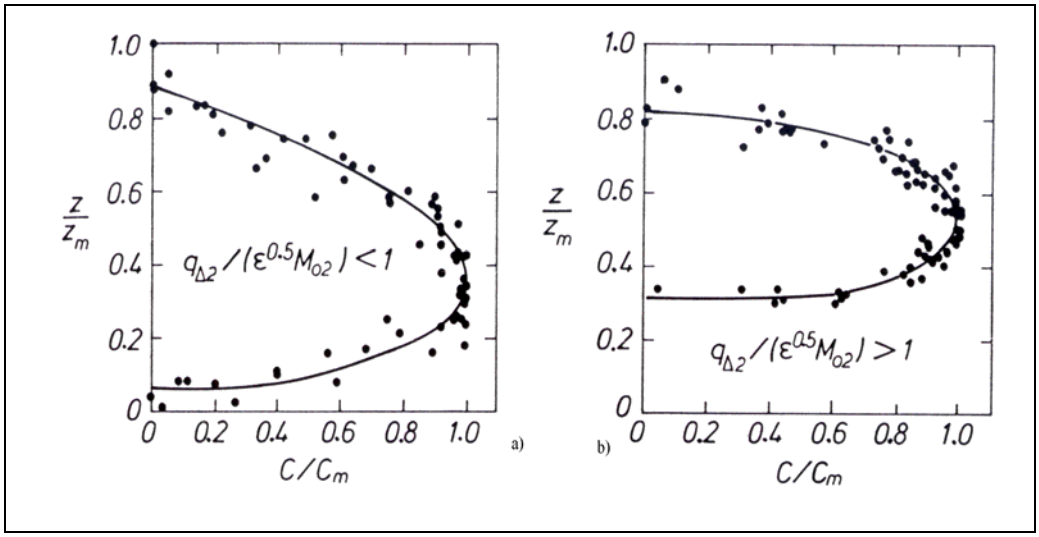

Figure 4.9: Concentrations in the spreading layer from a two-dimensional vertical jet in a linearly stratified fluid. **a)** momentum dominated flow. **b)** buoyancy dominated flow. C_m is the maximum concentration, and C is the locally measured concentration. From Wright and Wallace (1984).

Above the maximum height of rise, entrainment exists where the rising plume penetrates the spreading layer, and into the upper surface of the unsteady boil. Within the outward spreading layer, however, the plume is in an ambient fluid of approximately the same density as that in the rising flow, and at the centreline the density difference can be assumed to be constant, thus reducing the number of equations by one. The set of dimensionless equations governing the flow is then

$$\frac{dm_{V*}}{ds_*} = -\frac{4}{\pi} I'_{g'} \frac{b_p p_{s*}}{Fr_0^{\,2}} \frac{\partial g_a'_*}{\partial z_*} (z_* - z_{e*}) \tag{4.66a}$$

$$\frac{dm_{H*}}{ds_*} = 0 \tag{4.66b}$$

$$\frac{dz_*}{ds_*} = \frac{m_{V*}}{(m_{H*}^2 + m_{V*}^2)^{1/2}} \tag{4.66c}$$

$$\frac{dx_*}{ds_*} = \frac{m_{H*}}{(m_{H*}^2 + m_{V*}^2)^{1/2}} \tag{4.66d}$$

$$\frac{db_*}{ds_*} = k_s \qquad (4.66e)$$

Experiments performed by Wong (1985) in which buoyant jets were ejected horizontally show that the previous model underestimates the rise height by approximately 20% (figure 4.10) whereas it greatly overestimates the dilution for the jetlike phase of the flow (B / $N^{1/2}M$ < 2), as is seen in figure 4.11.

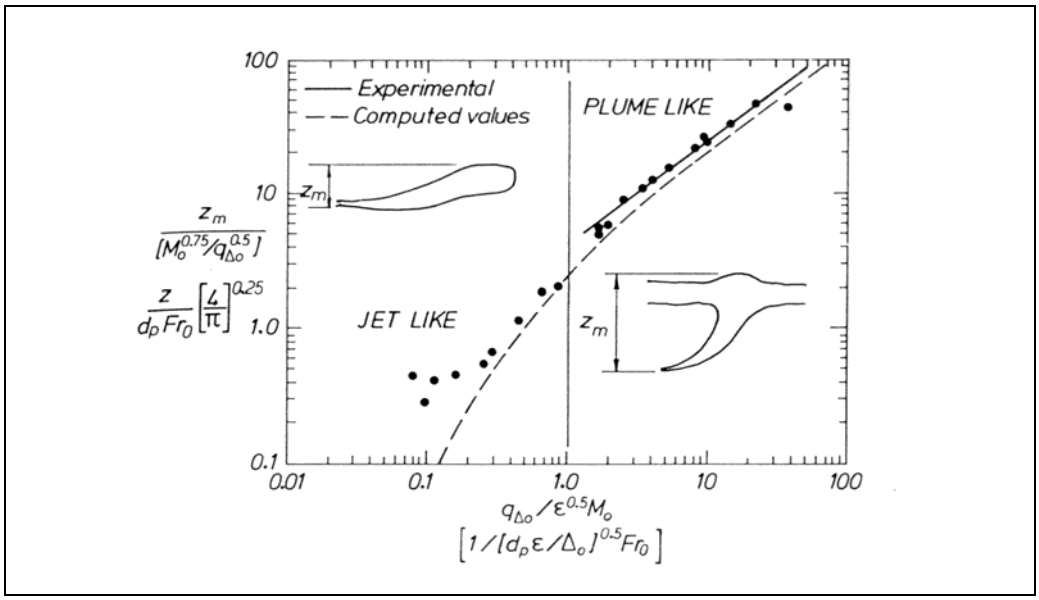

Figure 4.10: Dimensionless height of rise for an axisymmetric buoyant jet ejected horizontally into a stratified environment. From Wong (1985), in Wood *et al.* (1993).

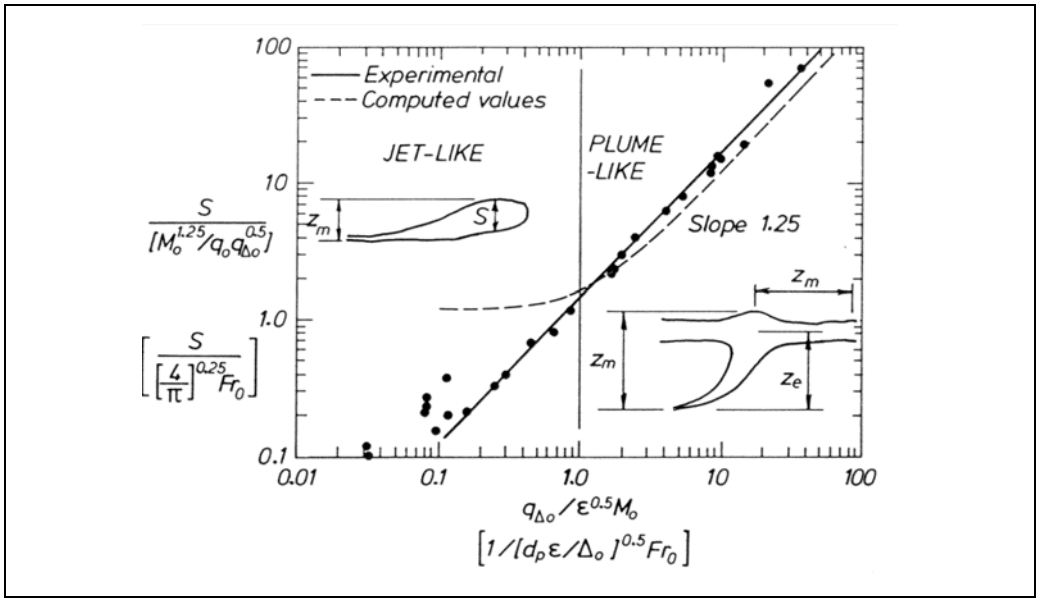

Figure 4.11: Dimensionless dilution for an axisymmetric buoyant jet ejected horizontally into a stratified environment. From Wong (1985), in Wood *et al.* (1993).

4.2.2 Ambient currents

Although the general behaviour of a single round buoyant jet in a stagnant environment is well established, the mixing of a deflected turbulent buoyant jet in a current field is a much more complicated problem, due to the interaction of the discharge velocity, the buoyancy-induced velocity, and the ambient velocity. However, since it has long been known that a submerged horizontal discharge into a perpendicular current gives better initial mixing than a vertical discharge or a horizontal discharge in still waters, an important effort has been done to understand and describe the jet motion in a moving environment; most of the work has been dedicated to the study of horizontal or vertical jets and plumes in cross- or co-flows (i.e., currents normal to, or in the same direction as, the discharge). Adams and Stolzenbach (1977), for instance, discovered that the mixing efficiency of a discharge depends on the basic current pattern, in addition to the diffuser type. As an example, staged diffusers optimised mixing in environments with strong bidirectional currents, whereas tee diffusers were best in the presence of weak bidirectional flows.

In the presence of a current, the initial discharge flow, usually a buoyant jet, is deflected after a certain time - which depends on the relative magnitude of the discharge and the ambient velocities, together with the angle between both parameters - by the drag as the current flows around the jet, and by the entrainment of ambient water having cross-flow momentum,. When the momentum flux of the discharge is small, the buoyancy flux becomes the relevant parameter. In the case of a momentum-driven discharge, a “momentum” lengthscale l_m can be defined, whereas if the discharge is driven by the initial buoyancy, a “buoyancy” lengthscale l_B can be introduced:

$$l_m = \frac{M^{1/2}}{U_a} \tag{4.67}$$

$$l_B = \frac{B}{U_a^3} \tag{4.68}$$

where U_a is the ambient velocity. The “momentum” lengthscale represents the distance from the discharge point at which a jet becomes strongly deflected by the crossflow, while the “buoyancy” lengthscale measures the vertical distance from the source at which the velocity induced by the buoyancy has decayed to the ambient velocity value, and the plume is thus advected. Both lengthscales are important in the study of current effects on effluent discharges, although Jirka and Lee (1994) and Wood *et al.* (1993) point out that, in practice, most artificial ocean discharges are governed mainly by the buoyancy flux and are little affected by the momentum flux and, hence, by the orientation of the discharge.

Wright (1977) has classified the flow of a jet in a uniform unstratified crossflow into four asymptotic regimes: a momentum-dominated near field, a buoyancy-dominated near field, a momentum-dominated far field, and a buoyancy-dominated far field, each one with its particular characteristics. Wood *et al.* (1993) find up to five possible flow regimes for an effluent in a current, depending on the relative magnitudes of the discharge velocity and the current velocity. These regimes are the advected strong jet, the weak jet, the momentum vortex, the advected plume and the advected thermal, and the flow may go from one regime to another as the initial momentum flux decreases; the transitions between each regime are defined by a set of lengthscales, which are not given here, but can be found in Wood *et al.* (1993).

One main feature of the effects of currents on an effluent is the transition from a Gaussian region, in which the velocity and buoyancy distributions are well described by a Gaussian function, to a vortex region in which the flow is similar to a vortex pair with distributed vorticity (figure 4.12). It is assumed that this transition is quite sudden, as supported by different observations (Wood *et al.*,

1993), and depends primarily on the local conditions at the transition point. When the distribution is Gaussian, the centreline concentration corresponds to the minimum dilution; however, in the vortex-like flow, the minimum dilution is not at the centreline. In any case, Andreopoulos and Rodi (1984) point out that the secondary motion that generates the pair of vortices decays in the downstream direction, due to the action of turbulent stresses.

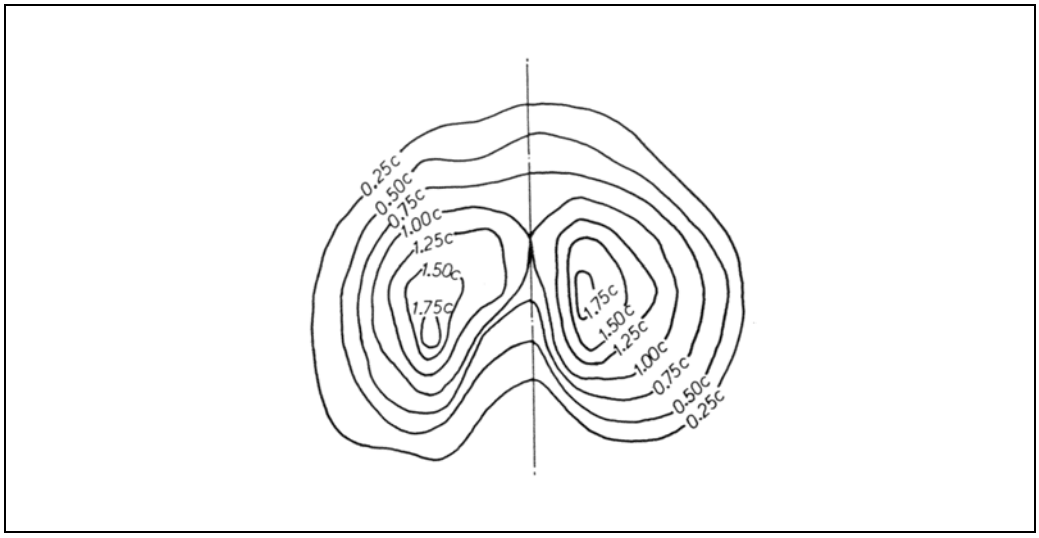

Figure 4.12: The concentration contours in an advected line thermal (Fan, 1967).

Fischer *et al.* (1979) attempted to obtain solutions for buoyant jets in ambient currents by developing asymptotic solutions for vertical jets and plumes in crossflows, and then assuming that the solution for buoyant jets was a combination of the former. In the case of a pure jet in a crossflow, the equations for the centreline velocity, tracer (or buoyancy) excess and trajectory are

$$\begin{cases} w_m \propto U_a\left(\dfrac{l_m}{z}\right) \\ C \propto D_1 \dfrac{U_a B}{Mg}\left(\dfrac{l_m}{z}\right) \\ \dfrac{z}{l_m} = C_1\left(\dfrac{x}{l_m}\right)^{1/2} \end{cases} \quad z \ll l_m \qquad (\text{jet}) \tag{4.69}$$

$$\begin{cases} w_m \propto U_a\left(\dfrac{l_m}{z}\right)^2 \\ C \propto D_2 \dfrac{U_a B}{Mg}\left(\dfrac{l_m}{z}\right)^2 \\ \dfrac{z}{l_m} = C_2\left(\dfrac{x}{l_m}\right)^{1/3} \end{cases} \quad z \gg l_m \qquad (\text{bent}-\text{over jet}) \tag{4.70}$$

whereas for the pure plume the equations become

$$\begin{cases} w_m \propto U_a \left(\frac{l_B}{z}\right)^{1/3} \\ C \propto D_3 \frac{U_a B}{Mg} \left(\frac{l_M}{l_B}\right)^2 \left(\frac{l_B}{z}\right)^{5/3} \\ \frac{z}{l_B} = C_3 \left(\frac{x}{l_B}\right)^{3/4} \end{cases} \quad z << l_B \qquad \text{(plume)} \tag{4.71}$$

$$\begin{cases} w_m \propto U_a \left(\frac{l_B}{z}\right)^{1/2} \\ C \propto D_4 \frac{U_a B}{Mg} \left(\frac{l_M}{l_B}\right)^2 \left(\frac{l_B}{z}\right)^{2} \\ \frac{z}{l_B} = C_4 \left(\frac{x}{l_B}\right)^{2/3} \end{cases} \quad z >> l_B \qquad \text{(bent-over plume)} \tag{4.72}$$

where the C_i and D_i are experimental coefficients.

In their study, they assumed that a buoyant jet will behave as a combination of the previous equations, depending on the ratio l_m/l_B, z/l_B, and z/l_m. An example is given in figures 4.13 and 4.14, where the buoyant jet will behave as a jet up to $z \approx l_m$, when it will start behaving like a plume, and from $z \approx l_B$ it will act like a bent-over plume.

For the limiting case of a vertical buoyancy-dominated discharge with $Fr_0 = 1$ (or $l_M/l_Q = (4/\pi)^{1/4}$), Wright (1977) offers the following expressions for the centreline dilution and the jet trajectory:

$$\begin{cases} \frac{SQ}{U_a l_B^{\,2}} = 0.42 \left(\frac{z}{l_B}\right)^{5/3} & z << l_B \\ \frac{SQ}{U_a l_B^{\,2}} = 0.41 \left(\frac{z}{l_B}\right)^{2} & z >> l_B \end{cases} \tag{4.73}$$

$$\begin{cases} \frac{z}{l_B} = 1.35 \left(\frac{x}{l_B}\right)^{3/4} & z << l_B \\ \frac{z}{l_B} = 0.85 \left(\frac{l_M}{l_B}\right)^{1/9} \left(\frac{x}{l_B}\right)^{2/3} & z >> l_B \end{cases} \tag{4.74}$$

Since for these conditions (Fr_0=1) the initial port orientation becomes unimportant, these sets of equations can also be used for horizontal discharges, in which the motion in the horizontal plane is driven by the jet momentum and the ambient current. Further, since the discharge imparts no vertical momentum, the motion in the vertical plane is determined primarily by the interaction of the discharge

buoyancy with the ambient flow. When Fr_0>1, the effect of the initial jet momentum is to increase the horizontal distance of travel before the buoyant discharge starts to rise vertically like a plume.

Lee and Cheung (1990) presented the following expressions to compute the centreline dilution for buoyancy-dominated jets in currents

$$\begin{cases} \dfrac{SQ}{U_a l_B^2} = 0.10\left(\dfrac{z}{l_B}\right)^{5/3} & z < 0.01\, l_B \\ \dfrac{S\,Q}{U_a l_B^2} = 0.51\left(\dfrac{z}{l_B}\right)^{2} & z \gg l_B \end{cases} \tag{4.75}$$

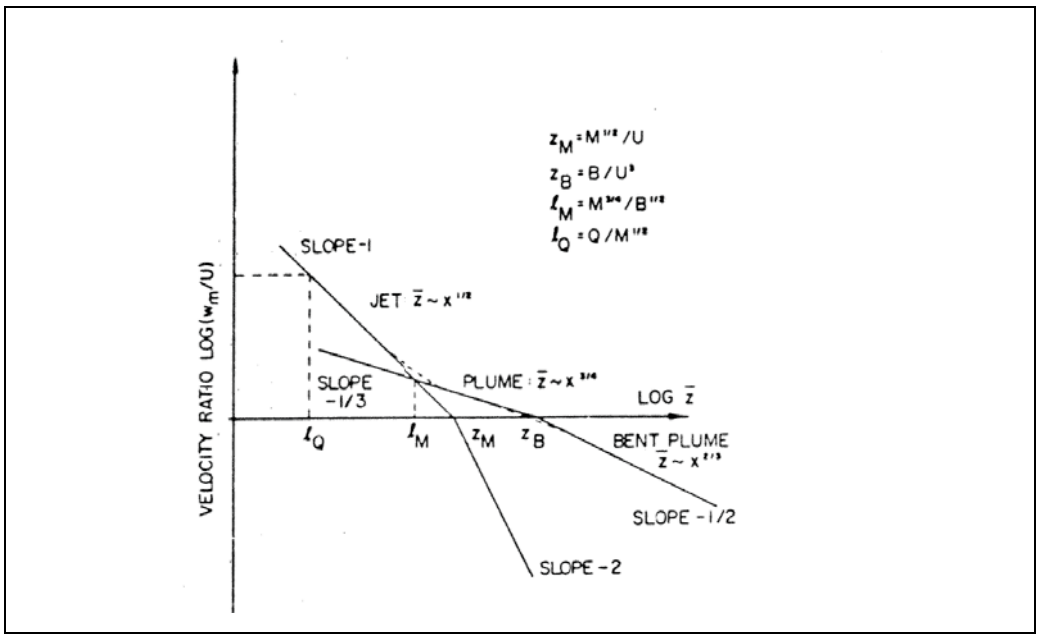

Figure 4.13: Vertical to horizontal mean velocity ratio in a turbulent buoyant jet in a uniform cross-flow (l_m<l_B), from Fischer *et al.* (1979). z_M and z_B in the figure are l_M and l_B in the text, respectively.

Alternative equations were supplied by Lee and Neville-Jones (1987), after interpreting a set of 320 field data points on initial dilution using lengthscale analysis, and finding that the minimum surface dilution of a horizontal buoyant jet in a cross-flow was

$$\begin{cases} S = 0.31\dfrac{B^{1/3}H^{5/3}}{Q} & z < 5l_B \\ S = 0.32\dfrac{U_a H^2}{Q} & z \geq 5l_B \end{cases} \tag{4.76}$$

in an unstratified fluid of depth H. They also provided an estimation for the time-averaged location of the sewage boil, as

$$z_{boil} = 1.1 \frac{H^{3/2} U_a^{3/2}}{B^{1/2}} \tag{4.77}$$

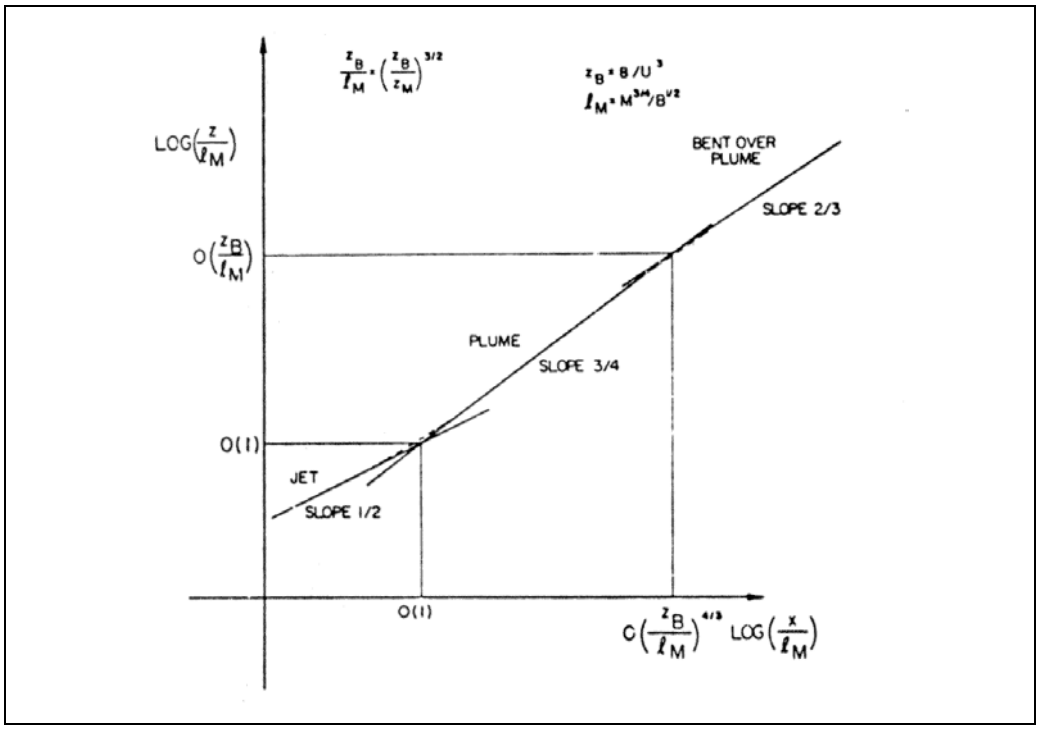

Figure 4.14: Jet trajectory in a uniform cross-flow ($l_m<l_B$), from Fischer *et al.* (1979). z_M and z_B in the figure are l_M and l_B in the text, respectively.

Each set of equations (4.75) and (4.76) describes plume dilution in two successive but different phases, namely the buoyancy-dominated nearfield (BDNF, in which the dilution does not depend on the ambient current) and the buoyancy-dominated farfield (BDFF, in which dilution does not depend on the initial buoyancy flux); however, a discontinuity appears in the transition region between both phases. Huang *et al.* (1998) attempted to find a continuous description of plume dilution, avoiding the transition discontinuity, and developed a model for initial dilution that yields a single equation for centreline dilution including the effects of shear and forced entrainment, as

$$\frac{SQ}{U_a z^2} = C_1 \left(\frac{z}{l_B} \right)^{-1/3} + \frac{C_2}{1 + a_1 \left(\frac{z}{l_B} \right)^{-a_2}} \tag{4.78}$$

with C_1 = 0.10, C_2 = 0.51, a_1 = 0.1 and a_2 = 2. In a similar way, they also obtain an equation for minimum surface dilution, taking into account the blocking effect of the established wastefield at the water surface,

$$\frac{SQ}{U_a H^2} = C_3\left(\frac{H}{l_B}\right)^{-1/3} + \frac{C_4}{1+a_3\left(\frac{H}{l_B}\right)^{-a_4}} \tag{4.79}$$

where $C_3 = 0.08$, $C_4 = 0.32$, $a_3 = 0.2$ and $a_4 = 0.5$. Both equations agree well with experimental data, as seen in figures 4.15a,b below:

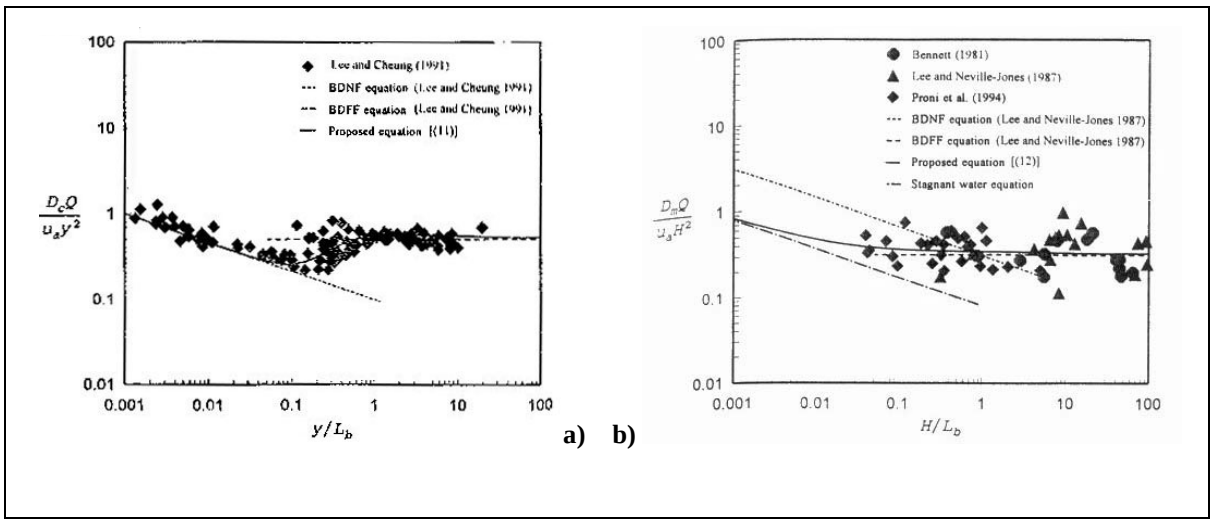

Figure 4.15: a) Centreline dilution for vertical jets, **b)** Minimum surface dilution for horizontal jets. From Huang *et al.* (1998).

Complete equations for jet momentum flux, buoyancy flux, dilution and jet trajectory were obtained by Wood *et al.* (1993), whose approach is based on finding the general equations for the initial flow assuming Gaussian velocity distributions, and those for the later flow with vortex-like distributions, and then looking at what happens in the transition region. For the Gaussian flow, they give the following equations for the momentum, the trajectory and the spread function, assuming the ambient flow is horizontal and the discharge is in the same direction, but at an angle θ_V from the horizontal:

$$\frac{d}{ds}\left[m_e \cos\alpha_r\right] = 0 \tag{4.80}$$

$$\frac{d}{ds}\left[m_e \sin\alpha_r\right] = I_{g'} g' b^2 \tag{4.81}$$

$$U_a \cos\alpha_r I_{g'} g' b^2 + I_\beta U_{eg} g' b^2 = B \tag{4.82}$$

$$\frac{dz}{ds} = \frac{U_{eg}\sin\alpha_r}{U_a \cos\alpha_r + U_{eg}} \tag{4.83}$$

$$\frac{dx}{ds} = \frac{U_a + U_{eg}\cos\alpha_r}{U_a \cos\alpha_r + U_{eg}} \tag{4.84}$$

$$\frac{db}{ds} = \frac{k_s U_{eg}}{U_a \cos\alpha_r + U_{eg}} \tag{4.85}$$

where

$$m_e = I_m U_{eg}^2 b^2 + U_a \cos\alpha_r I_q U_{eg} b^2 \tag{4.86}$$

and U_{eg} is the velocity at which the jet centre moves relative to the current, α_r is the angle between U_a and $U_{eg,}$ and I_q is a new shape function defined as

$$I_q = \int_0^\infty \frac{u_{eg}}{U_{eg}} 2\pi \frac{r}{b} d\left(\frac{r}{b}\right) \tag{4.87}$$

with u_{eg} the excess velocity off the centreline, assuming a Gaussian distribution. On the other hand, the equations for the vortex-like flow region are

$$m = \left[\frac{Bt}{U_a} + m_T \sin\alpha_{rT}\right]^2 + \left[m_T \cos\alpha_{rT}\right]^{1/2} \tag{4.88}$$

$$\frac{db}{dt} = a_m U_{ev} = \frac{a_m m}{I_v b^2 \sin\alpha_r} \tag{4.89}$$

$$\frac{dz}{dt} = U_{ev} \sin\alpha_r \tag{4.90}$$

$$\frac{dx}{dt} = U_a + U_{ev} \cos\alpha_r \tag{4.91}$$

where a new shape function has been defined as

$$I_v = \int_0^\infty \frac{u_{ev}}{U_{ev}} \frac{1}{b^2} dA \tag{4.92}$$

with A an area, U_{ev} the velocity at which the vortex pair is moving through the ambient flow, and u_{ev} the local vortex–induced velocity. Here, the subindex T represents the value of the properties at some known time.

In the transition region, the equations for the momentum and buoyancy fluxes are given by (Wood *et al.*, 1993)

$$I_v U_{ev} b^2 \sin\alpha_{rT} = \frac{m_{eT}}{U_a} \tag{4.93}$$

$$I_{\Delta v} g' b^2 \sin\alpha_{rT} = \frac{B}{U_a} \tag{4.94}$$

with $I_{\Delta v}$ the shape function

$$I_{\Delta v} = \int \frac{g_L}{g_v} \frac{1}{b^2} dA \qquad (4.95)$$

and where g_v is the characteristic buoyancy in the vortex pair, and m_{eT} and α_{rT} are the excess momentum in the Gaussian region before the transition and the angle relative to the ambient current of the Gaussian flow, respectively.

Wood *et al.* (1993) also present an analysis for the general situation in which the effluent is discharged at an arbitrary angle to the ambient current. For the Gaussian distribution region, equations (4.80), (4.81), (4.82), (4.83) – now *dy*/*ds* -, (4.84), (4.85) are still valid, after replacing $cos\alpha_r$ with $cos\alpha_r cos\sigma_r$, where σ_r is the angle between the projection of the relative velocity U_{eg} on the horizontal plane and the ambient current (figure 4.16). An additional equation for the trajectory must be introduced, since the flow will now be three-dimensional:

$$\frac{dz}{ds} = \frac{U_{eg} \cos\alpha_r \sin\sigma_r}{U_a \cos\alpha_r \cos\sigma_r + U_{eg}} \qquad (4.96)$$

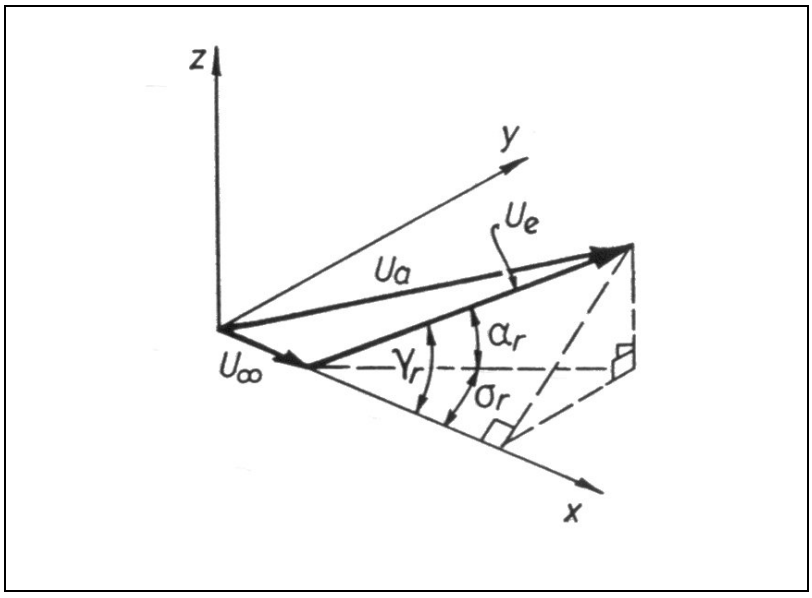

Figure 4.16: Variables for the case of a discharge flow at an arbitrary angle to the ambient flow (from Wood *et al.*, 1993).

For the vortex-like flow region, the momentum flux equation (4.88) is still valid after replacing $sin\alpha_r$ and $sin\alpha_{rT}$ with $sin\gamma_r$ and $sin\gamma_{rT}$, respectively, with γ_r the angle between the relative velocity and the ambient current; the spread equation remains unchanged, and the trajectory equations (4.90) and (4.91) –now *dy*/*dt* – are also valid, changing only $cos\alpha_r$ by $cos\alpha_r cos\sigma_r$. Again, a new equation must be introduced to account for the three-dimensionality of the flow:

$$\frac{dz}{ds} = U_{ev} \cos\alpha_r \sin\sigma_r \qquad (4.97)$$

The final characteristics of the wastefield depend on the combination of the effects of both the current field and the waterbody stratification. Figure 4.17 shows the flow pattern for a buoyant jet

rising through a flowing stratified fluid; the flow in 4.17a corresponds to a stagnant stratified field, discussed in §4.2.1. The main assumption in this case is that above the equilibrium level the rising flow is surrounded by an outflowing effluent field of similar dilution to that on the plume centreline.

For the other types of flow, however, this assumption is no longer valid. As the ambient current increases, the plume becomes stretched in the horizontal direction, so that the equilibrium effluent field that surrounds the plume when U_a is small is swept downstream. For the flows of the type depicted in figure 4.17b, as the wastefield is swept away, ambient fluid entrainment will occur above the equilibrium level at least over a portion of the plume surface, so that there are two levels at which the density in the rising plume equals the ambient density: the first in the plume rise, and the second above the equilibrium level. When the ambient current is large relative to the buoyancy-induced momentum, the effluent flow is similar to that in figure 4.17c, in which the vertical distance between the maximum rise height z_t and the equilibrium height z_e is relatively small.

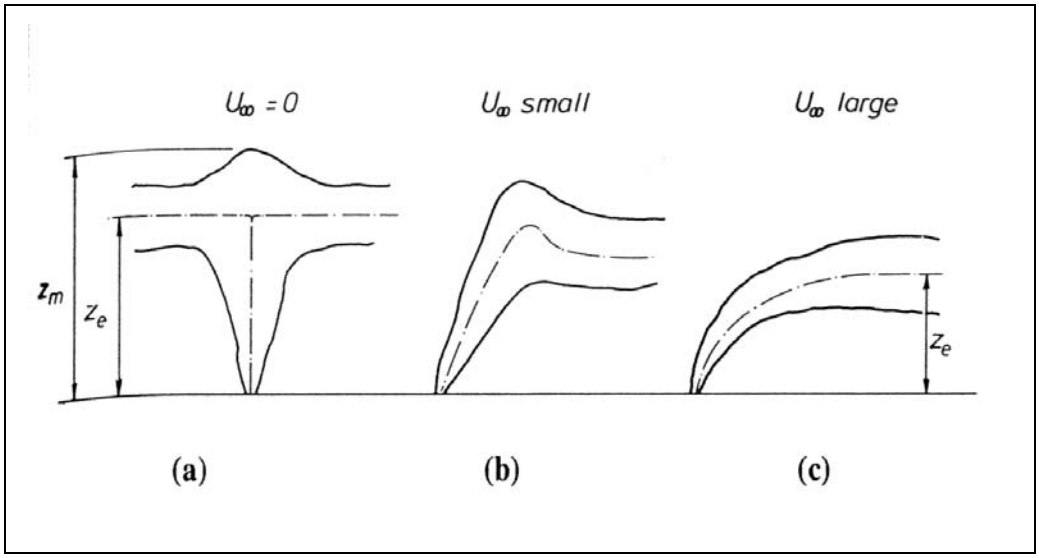

Figure 4.17: Flow patterns for a buoyant jet rising in a flowing stratified fluid (from Wood *et al.*, 1993).

The modelling of effluent behaviour in a moving stratified environment presents some difficulties that did not arise when the waterbody was uniform. In the latter situation, the constant functions appearing in the numerical model given by Wood *et al.* (1993) appeared to vary depending only on the establishment of a vortex pair, which remains approximately normal to the plume's axis. Under conditions of water stratification, the vortex behaviour may be changed, and the way in which the shape constants vary with the crossflow may also be altered; in a similar manner, the transition between the Gaussian and the vortex regions may be affected by the stratification. However, Wright (1977) carried out a set of experiments in which he towed a vertical buoyant jet in a stratified fluid and reached the conclusion that, up to the maximum height of rise, the trajectory of the jet was approximately given by the unstratified trajectory, so the corresponding equations from §4.2.2 can be used. A general numerical model, with equations that include additional terms due to the flux of buoyancy from the ambient current, is presented in Wood *et al.* (1993).

On the other hand, Fischer *et al.* (1979) present a set of asymptotic solutions for trajectory and dilution, based on those given for buoyant jets in a moving unstratified fluid, but substituting the horizontal distance in the trajectory equations with a new parameter λ, defined as the horizontal wavelength of the vertical oscillations of the moving plume that are supported by the density stratification,

$$\lambda = \frac{U_a}{N^{1/2}} \qquad (4.98)$$

together with estimations of the terminal height of rise, depending on the importance of the influence of the buoyancy and the ambient current on the jet.

4.3 MIXING REGIONS: THE NEARFIELD, THE FARFIELD, AND THE ZONE OF WASTEFIELD ESTABLISHMENT

The mechanisms that govern the mixing of a discharge from a marine outfall are not the same during all the dispersion process, but vary with the distance to the source. Based on this fact, most researchers divide the process of substance dispersion into two main phases, namely the *nearfield* and the *farfield*, depending on the physical mechanisms that dominate the mixing process. Some authors (e.g., Koh and Brooks, 1975; Fischer *et al.*, 1979) prefer to add a third phase they call the *zone of wastefield establishment* between the former two, and define it as a region of transition where the discharge abandons the nearfield and enters the farfield; Tsanis and Valeo (1994), however, consider this third region as the end part of the nearfield.

Roberts (1979) describes the dispersion process as existing in three separate phases: first, there is an initial dilution phase, in which the buoyancy and momentum of the discharge and the dynamic effect of the local current result in rapid mixing and dilution of the effluent with the ambient water. Second is a phase consisting of dynamic horizontal spreading and vertical collapse of the wastefield after reaching its terminal height of rise, which may be below the water surface if the water stratification is strong enough. The last phase of effluent transport consists of dynamically passive turbulent diffusion and advection by ocean currents.

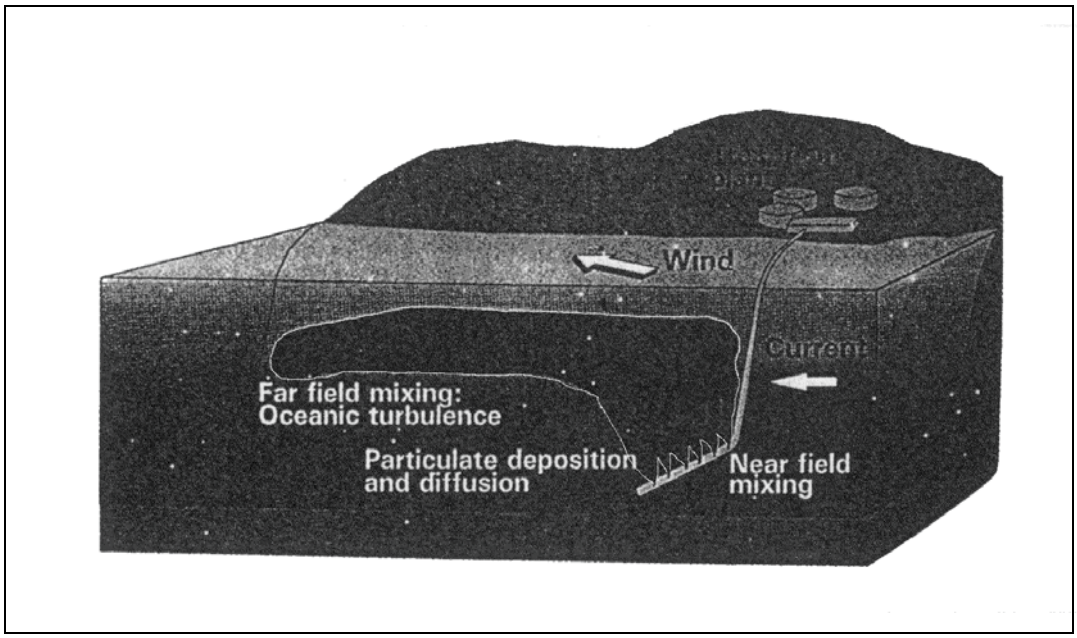

Figure 4.18: Typical behaviour of pollutant discharged from an ocean outfall (from Roberts, 1994).

These different regions are illustrated in figure 4.18, which shows the typical behaviour of an outfall discharge. To maximise dilution, the sewage is usually disposed of as a horizontal jet, which rapidly becomes a plume rising towards the surface because of its density deficiency with respect to the surroundings. During this phase -the nearfield-, the mixing is rapid, and is due to the turbulence generated by the discharge itself (Roberts, 1994). The sewage will reach the surface or a level of neutral buoyancy if the waterbody is stratified, and will start to spread horizontally and collapse vertically because of gravity; this region is the so-called zone of wastefield establishment. After the wastefield has been established, it will diffuse and drift with oceanic turbulence and the ocean currents. In this last phase -farfield- some particles may deposit on the ocean floor due to differential settling and turbulent diffusion.

The emphasis with which dispersion must be treated in each one of these regions depends on the type of released substance. In the case of a discharge rich in biological agents (bacteria, for instance), it is important to perform an accurate modelling of the nearfield region, because bacteria decay rapidly in an oceanic environment and only a relatively small percentage of the discharged population will remain active when the farfield begins. On the other hand, if the pollutant contains mercury or radioactive elements, the farfield modelling is important, because even small concentrations of these elements away from the source present high levels of toxicity.

4.3.1 The Nearfield

The nearfield, or initial mixing zone, is defined as the region in the neighbourhood of the discharge point in which the mixing of the pollutant is effected by the buoyancy and momentum fluxes at the source, and by their interaction with the ambient current. The momentum and buoyancy of the discharge modify the ambient flow pattern, and the discharge generates its own mean velocity and turbulent flows. For the particular case of a marine outfall, the behaviour of the discharge in this region is highly affected by its design, and is thus not subjected to water quality standards (Tsanis and Valeo, 1997). The spatial scale of the nearfield is of the order of 10 m, with time scales of the order of minutes to one hour (Jirka and Lee, 1994), and the effluent dilution at the end of this region is called initial dilution.

In the nearfield, the discharge behaves like a turbulent buoyant jet, i.e., a submerged jet with an initial buoyancy that continues to drive it upwards and tends to make the columnar flow similar to that of a pure plume. In fact, according to Tsanis and Valeo (1994), the nearfield encompasses the buoyant jet flow and any surface, bottom or terminal layer interaction.

This region is usually treated using simple empirical formulae like those found by Cederwall (1968), Abraham (1963) and others, or by means of direct solutions to the integral transport equations based on the ideas of Morton *et al.* (1956) or Fan and Brooks (1969), and developed extensively in Fischer *et al.* (1979).

For marine outfalls, the study of the nearfield behaviour of buoyant discharges is commonly divided, for the sake of simplicity, into two parts.

a) First, the buoyant jet originating at each outfall diffuser is treated individually; since the outlets are normally round ports, the discharge is governed by the properties of round buoyant jets and plumes, a summary of which as been given previously, and can be found in Fischer *et al.*(1979) and Wood *et al.* (1993). This is the only stage of the dilution process which is under control of the outfall designer, and it is also where most of the dilution takes place.

b) Second, the individual buoyant jets merge, a short time after the discharge, above the outfall, generating a single pollutant field. The properties of the resulting two-dimensional plume have also been given in this chapter, and can be found in the references mentioned above.

A general, and alternative, analysis of the nearfield properties (and, in particular, the behaviour of the jet or plume) can be carried out by defining the important dynamic variables of the discharge using the most relevant diffuser and oceanographic parameters. The former are the jet velocity w_0, the port diameter d_p, and spacing p_s, and the density difference between effluent and seawater $\Delta\rho$, whereas the latter are the ambient current speed U_a, and its direction relative to the diffuser θ_d, and the density stratification. The dynamic variables of interest are (Jirka and Doneker, 1991) the kinematic momentum flux $M=w_0Q$, the kinematic buoyancy flux $B=g_0'Q$ and, to a lesser extent, the source discharge, or volume flux, Q.

A dimensional analysis of these three fluxes leads to the definition of seven length scales (Jirka and Doneker, 1991; Fischer *et al.*, 1979), some of which have been defined before and used in this chapter, that describe the behaviour of the discharge:

$$l_Q = \frac{Q}{M^{1/2}} \qquad l_M = \frac{M^{3/4}}{B^{1/2}} \qquad l_m = \frac{M^{1/2}}{U_a} \qquad \text{(4.99 a-c)}$$

$$l_B = \frac{B}{U_a^3} \qquad l_T = \frac{M^{2/3}}{(BU_a)^{1/3}} \qquad \text{(4.99d-e)}$$

$$l'_m = \frac{M^{1/4}}{N^{1/4}} \qquad l'_B = \frac{B^{1/4}}{N^{3/8}} \qquad \text{(4.99f-g)}$$

where N is defined in equation (4.42).

Equation (4.99a) defines the discharge length scale, which is a measure of the initial jet size and the length of its flow establishment, and is equal to the square root of the port sectional area a_0. l_M is a measure of the distance at which the behaviour of the discharged jet becomes plumelike in a stagnant environment (jet/plume transition length scale), whereas l_m (jet/cross-flow length scale) measures the distance from the source beyond which the jet becomes strongly deflected by a cross-flow; in the case of a flow in the same direction as the jet, l_m determines the length of the jet region. Equation (4.99d) defines the plume/cross-flow transition length scale, which is the vertical distance the plume will rise (or fall) before becoming advected by the cross-flow. The length scale l_T measures the transition between the stages that are influenced by momentum or by buoyancy. The two latter length scales, l'_m and l'_b are a measure of the distance at which a jet or a plume, respectively, are affected by stratification (in a stagnant, linearly stratified ambient), leading to pollutant trapping and horizontally spreading flows.

However, only four of these seven variables are independent, and are used to characterise the behaviour of pollutant discharges in stratified flows (Jirka and Doneker, 1991). These authors define up to 35 flow classes, based on the values of (4.99a-g), into which all possible flow configurations can be classified. A similar analysis is performed for multiport discharges in Jirka and Akar (1991), where six relationships, analogous to (4.99a-g), are defined considering a slot (2D) plume.

4.3.2 The Zone of Wastefield Establishment

The zone of wastefield establishment is the intermediate region between the nearfield and the farfield, and is characterised by the transition from the vertical plume flow to a horizontal spreading motion generated by the gravitational collapse of the pollutant cloud; the flow structure in this region is therefore dominated by horizontal motions and possible interfacial shear at pycnoclines.

Even though this transition phase is not yet well described in the literature, and is generally neglected in the development of numerical transport models, it is possible to determine some properties of the established wastefield which can then be used as initial conditions for farfield modelling. According to Roberts (1994) the most important established wastefield features are the rise height z_t, the height to the level of minimum initial dilution z_e, the thickness h_e and the minimum initial dilution S_0, although other variables are also required to enable coupling to a farfield model, such as the width b_e of the wastefield, the length of the initial mixing region L_i , and the spatial variation of the pollutant concentration $C(y,z)$ over a vertical plane at the end of the flow establishment region (fig. 4.19). The subindex e in these variables stands for "equilibrium level", i.e., where the density difference between the effluent and the ambient water disappears

The terminal height of rise of a buoyant jet in a linearly stratified and stagnant ambient has been given before –equation (4.44)-, from Fischer *et al.* (1979). The correct prediction of this height is important for several reasons. In the first place, it governs the elevation in the water at which nutrients and pathogens settle; secondly, it also affects bacterial die-off, which depends strongly on sunlight; and, finally, ambient current speed and direction (which dictate farfield transport) may vary significantly over depth, especially under stratified conditions when internal waves can be present. The same authors point out that mixing above the bottom plume surface only serves the purpose of evening out the concentration differences existing within the plume. They also offer an estimation of the wastefield thickness, assuming that the width b_e of the wastefield normal to the crossflow, the average dilution S_a at the top of the wastefield, and the terminal height of rise are known

$$h = z_t \left[\frac{QS_a / U_a b_e z_t}{1 + QS_a / U_a b_e z_t} \right] \tag{4.100}$$

where, in the case of a uniform ambient,

$$S_a = 0.54 \left(\frac{(g'_0 q)^{1/3} z_t}{q} \right) \tag{4.101}$$

$$b_e = C_b (g'_0 q)^{1/3} \frac{L_d}{u_a} \tag{4.102}$$

:

$$\begin{cases} S_{aw} = \dfrac{0.38 (g'_0 q)^{1/3} z_t}{q} & \text{parallel current} \\ S_{aw} = S_a \left(1 + \dfrac{QS_a}{u_a b z_t} \right) & \text{perpendicular current} \end{cases} \tag{4.103}$$

with C_b about 1.2, and S_{aw} the average dilution in the wastefield. For a stratified environment, the effects of blocking by the submerged wastefield on the rising plume must be taken into account, and the following equations are given:

$$b = C_{b'}\left(Nq^2\right)^{1/4}\frac{L_d}{u_a} \tag{4.104}$$

$$S_a = \sqrt{2}\left(0.31\frac{g_0'^{1/3} z_t}{q^{2/3}}\right) \tag{4.105}$$

$$\begin{cases} S_{aw} = S_a - A\sqrt{\dfrac{A^2}{4} + S_a} + \dfrac{A^2}{2} & \text{parallel current} \\ S_{aw} = S_a\left(1 + \dfrac{QS_a}{u_a b z_t}\right) & \text{perpendicular current} \end{cases} \tag{4.106}$$

with

$$A = \frac{S_a\left(Q/L_d\right)^{1/2}}{z_t 0.8N^{1/4}} \tag{4.107}$$

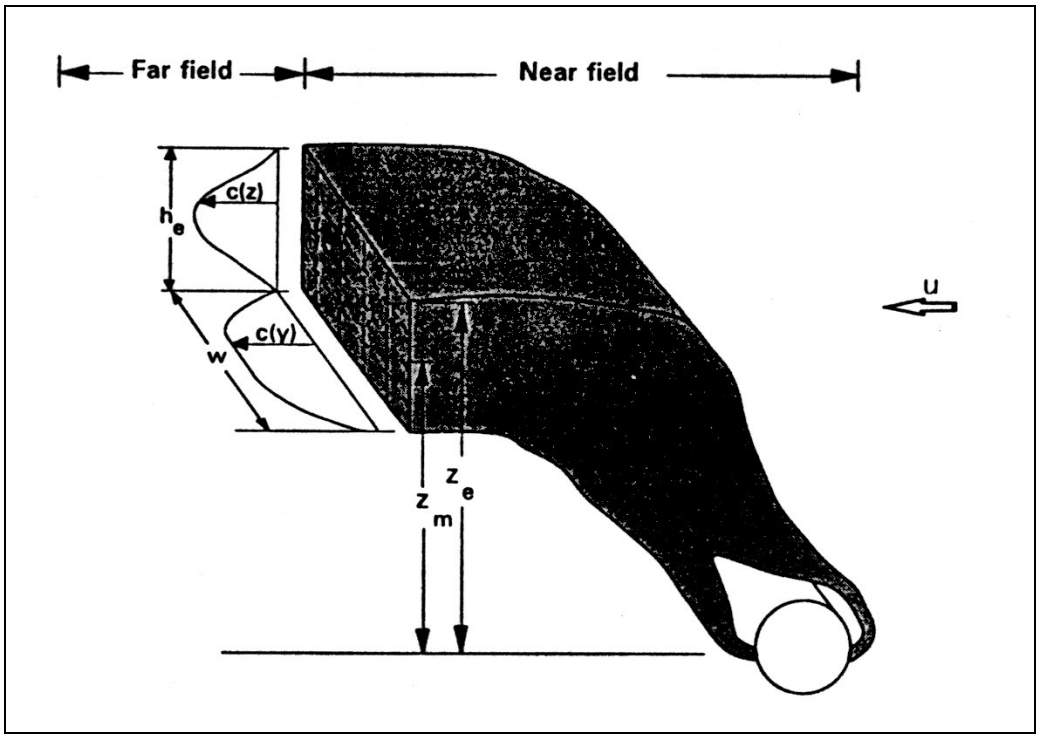

Figure 4.19: Principal characteristic parameters of the zone of wastefield establishment (from Roberts, 1994). Here, z_m and z_e refer to equilibrium and terminal rise height, respectively, (z_e and z_t in the text).

Roberts and co-workers presented in 1989 the results of a series of experiments performed in an attempt to describe the formation and evolution of submerged wastefields (Roberts *et al.*, 1989a,b,c). After defining three new lengthscales -equivalent to (4.99a, b and g), respectively, although now the initial variables Q, M, and B are per unit diffuser length of volume-

$$l_{QR} = \frac{Q_L^2}{M_L}$$
$$l_{MR} = \frac{M_L}{B_L^{2/3}} \qquad (4.108a\text{-}c)$$
$$l_{BR} = \frac{B_L^{1/3}}{N}$$

they decided to perform their experiments in the range $0<Fr_0<100$, $0.078 \le l_{MR}/\, l_{BR} \le 0.5$ and $0.31 \le p_s/l_{BR} \le 1.92$, where $Fr_0=U_a^3/\beta$ is a Froude number and β is the buoyancy flux per diffuser unit length, which they said were typical conditions for actual ocean outfalls.

They proposed equations for the minimum initial dilution -i.e., minimum dilution at the end of the nearfield- and the rise height in a crossflow. They found that dilution did not depend on the current when the Froude number was smaller than 0.1, but did increase with current speed for larger Fr_0, and it was significantly larger for currents perpendicular to the outfall than for parallel ones. The expression they gave is

$$\frac{S_m Q_L N}{\beta^{2/3}} = \begin{cases} 0.97 & Fr_0 \le 0.1 \\ 2.19 Fr_0^{1/6} - 0.52 & 0.1 \le Fr_0 \le 100 \end{cases} \qquad (4.109)$$

where N is now the Brünt-Väisälä frequency ($N = (-g/\rho_0\, \partial\rho/\partial z)^{1/2}$).

When calculating the terminal height, the wastefield thickness and the height of the level of minimum dilution, they first observed that these variables did not differ significantly for currents at 90º and 45° relative to the discharge direction, but were greater for parallel currents. In a stagnant environment they proposed

$$\frac{z_t}{l_{BR}} = 2.6 \quad ; \quad \frac{h_e}{l_{BR}} = 1.8 \quad ; \quad \frac{z_e}{l_{BR}} = 2.6 \qquad (4.110)$$

for the line plume case. For $0 < Fr_0 \le 1$ (weak current) both the rise height and thickness increase slightly, whereas for $1 \le Fr_0 \le 100$ the following expressions apply

$$\frac{z_t}{l_{BR}} = 2.5 Fr_0^{-1/6} \quad \frac{z_e}{l_{BR}} = 1.5 Fr_0^{-1/6} \qquad (4.111)$$

for perpendicular currents.

They also gave an expression to calculate the lateral spreading rate in the case of parallel currents which is independent of the terminal rise height

$$\frac{\beta_e}{L_d} = C_1 \frac{x}{L_d} Fr_0^{-1/3} \tag{4.112}$$

with L_d the diffuser length, and they observed that the rate of spreading was higher in unstratified (C_1=1.2) than in stratified flows (C_1=0.70). For perpendicular currents, they concluded that the spreading rate was

$$\frac{\beta_e}{L_d} = 1 + 0.17 \left(\frac{x}{l_{BR}} Fr_0^{-1/3} \right)^{1/2} \tag{4.113}$$

but they remarked that this equation should be used with care due to the experimental uncertainty of their measured data. Their set of papers on ocean outfalls (Roberts *et al.*, 1989a,b,c) constitute a very exhaustive and complete analysis of the formation and evolution of submerged wastefields, including the effects induced by the design of the diffusers.

4.3.3 The Farfield

The farfield (or passive dispersal region) is the last phase that can be distinguished in the transport of marine outfall discharges, and it is characterised by advection from oceanic currents and passive ambient diffusion. While the general circulation is the governing mechanism for the bulk transport of the pollutant, its mixing with the ambient water is driven mainly by oceanic turbulent processes. According to Jirka and Lee (1994), the spatial scale of the farfield is of up to tens of kilometres, with timescales ranging from several hours to days.

The dispersion in the farfield is usually modelled using a Fickian approach, i.e., the process is characterised by eddy diffusion coefficients. Only two diffusivities are generally used, one describing the diffusion in the horizontal plane, and one in the vertical direction. The ratio between D_H and D_V is of the order of 10^6 (Ozmidov, 1990), but this value may vary in time, from place to place, and depend on the averaging scale of those horizontal and vertical processes for which the transport coefficients are to be determined. A review of extensively used dispersion coefficients can be found in a preceding section (§2.3.1.1).

However, the detail of a farfield calculation can vary considerably from case to case, depending on the complexity of the coastal environment, the availability of data, and the severity of the pollutant problem (Jirka and Lee, 1994). Thus, in the presence of a predominantly alongshore current, an effluent discharged at a short distance from the coast could be brought shoreward by lateral diffusion, requiring a rather accurate modelling in order to predict the possible effects of pollution at the shore. As an example of expressions applied in the farfield, the following equation, which is expected to hold for $SQ / U_a L_d z_t \leq 2$, is used to estimate the depth of the wastefield in a moving stratified water, for a line diffuser normal to a current:

$$h = z_t \left[\left(\frac{QS}{U_a L_d z_t} \right) \Big/ \left(1 + \frac{QS}{U_a L_d z_t} \right) \right] \tag{4.114}$$

where z_t and S are obtained from the corresponding nearfield equations (e.g., equations (4.49) and (4.48), respectively).

4.4 CONCLUSIONS

Marine outfalls are perhaps the only water polluting sources that can be tailored to suit human requirements before operating. For this reason, they have become the most widespread way of introducing domestic and/or industrial polluting substances into waterbodies, and an accurate description of their discharge characteristics, and the evolution of the resulting plume under different environmental factors, has become of great importance for coastal waters quality assessment.

The behaviour of any discharge in a waterbody depends on a large number of factors, such as the initial momentum, the initial buoyancy of the discharge, the depth at which the discharge occurs, the configuration of the ports, the outfall configuration, the orientation of the discharge with respect to ambient currents, the receiving waterbody density profiles, etc. All of these must be taken into account when designing marine outfalls in order to minimise the environmental impact of the discharge, and must also be considered when developing numerical models.

This chapter has introduced the different types of flow (jets, plumes, and buoyant jets) that can result from general discharges into the marine environment, depending on the initial conditions, mainly on the relative magnitude of the momentum and buoyancy fluxes. The characteristics of each flow type, such as the centreline velocity and dilution, trajectory and spread, depend on a distinct set of equations which involve different initial parameters.

Moreover, design parameters, such as the discharge depth and the outfall port separation, amongst others, and environmental factors, such as the predominant current fields and the density gradients, are shown to play an important role in the dispersion and later evolution of the discharge. These are responsible for the merging of individual jets or plumes rising from separated ports, for the deflection of the discharge, and the possible subsurface trapping of the wastefield, respectively, which are relevant variables in order to estimate the trajectory of the wastefield and its dilution.

Finally, and following the main trend in the literature, the pollutant dispersion process has been divided into three different regions, depending on whether the dominant dispersion mechanisms are clearly source-related (nearfield) or ambient-related (farfield), or whether they are related to both source and environment (waste establishment or transition zone). Each zone is described and treated in detail.